Progress Report

EXPERIMENTAL AND ANALYTICAL STUDIES OF CONTINUOUS LAPPED Z-PURLINS UNDER GRAVITY LOADING

Submitted to
Star Manufacturing Company
8600 South Interstate 35
Oklahoma City, Oklahoma

by

Benjamin Wallace

and

Thomas M. Murray, P.E.
Professor-in-Charge
Fears Structural Engineering Laboratory

Fears Structural Engineering Laboratory
School of Civil Engineering and Environmental Science
University of Oklahoma
Norman, Oklahoma

July, 1980

TABLE OF CONTENTS

LIST OF FIGURES

LIST OF TABLES

INTRODUCTION

The analysis procedure suggested in Reference 1 was developed and experimentally verified assuming the controlling failure mode in continous lapped Z-purlin roof framing systems was web buckling immediately outside the lap. The experimental testing program was limited to cantilever lap tests designed to eliminate all failure modes except web buckling. To ascertain the applicability of the suggested procedure for the design of continous Z-purlin systems and to verify the correctness of the solution for other than cantilever lap conditions, a testing program involving full scale purlin systems was conducted. This report summarizes the analytical and experimental results of five full scale purlin tests.

The testing program consisted of three two-span tests and two three-span tests; all spans of equal length. In each test, two lines of standard 8 x 3 Z-purlins as cold-formed by Star Manufacturing Company, Oklahoma City, Oklahoma were used. The purlins were placed with top flanges facing outward and steel roof deck was screwed directly to the top flanges with self-drilling fasteners. Distributed loading was applied with concrete blocks placed on the steel deck. The purlins were fully instrumented to provide test data for comparison with the analytical predictions.

The analysis procedure suggested in Reference 1 considers the purlin to be laterally restrained at the deck location and accounts for non-principal axis bending through the use of a ficticious horizontal load placed at the flange

opposite to the deck connection. Calculations are simplified by using a transformed section where the lip and flange on the deck side are considered to be concentrated at the top of the web. In the proposed method, rotational restraint of the deck is neglected and the resulting normal stress distribution is given by

$$\sigma_z = -M_x \frac{I_{xyb}}{I_{xt}} \left(\frac{I_{xt} X_t}{I_{xt} I_{yt} - I_{xty}^2}\right) + M_x \frac{I_{xyb}}{I_{xt}} \left(\frac{I_{xyt} Y_t}{I_{xt} I_{yt} - I_{xyt}^2}\right) + \frac{M_x Y_t}{I_{xt}} \quad (1)$$

where x- and y- are non-principal, centroidal axes with y parallel to the web and positive in the direction of the deck, I_x and I_y are moments of inertia, I_{xy} is the product of inertia and the subscripts t and b refer to the transformed section and a portion of the cross section consisting of the web and flange opposite the deck, respectively.

It is also suggested in Reference 1 that the critical web buckling stress can be computed using the stress distribution from Equation 1 and the provisions of Section 3.4.3 of the AISI specification for the design of cold-formed members (2). To obtain a predicted failure load, this stress is increased by the factor 1.67 which is the implied factor of safety in the AISI specification.

Experimental data from the testing program are compared to the analytical prediction in the following sections. Where necessary, modifications to the previously proposed method are suggested.

DETAILS OF EXPERIMENTAL PROCEDURES

A schematic of the two span test setup is shown in Figure 1; the three span setup is identical with the addition of the third span. For all tests the span length was 25 ft. 0 in.

The purlins were oriented with top flanges opposed and pointing outwards. At intermediate rafter locations, the purlins were lapped 1 ft. 2 in. on each side of the centerline of the rafter except for the outside spans of the three span condition where the exterior lap was 1 ft. 2 in. and the interior lap was 2 ft. 4 in. Near the end of each lap, two ½ in. diameter machine bolts were used to connect adjacent webs. Lengths of cold-formed roof sheeting 3 ft. wide by 6 ft. long were attached to the top flanges of the purlins using self-drilling fasteners (without washers) at approximately 1 ft. centers.

Initially the purlins were bolted directly to the top frame flange of the rafters which were in turn bolted to support beams. These beams were parallel to the purlins which effectively prevented movement of the rafters, and hence the purlin to rafter connection. Results of the first two-span test indicated that this arrangement caused cantenary tensile forces to be developed in the purlins which increased the load carrying capacity of the purlins. Since this degree of longitudinal rigidity in the test setup is not found in actual construction, e.g. rafters in rigid frames are essentially free to move in a direction parallel to the purlins except at a braced bay, modifications were

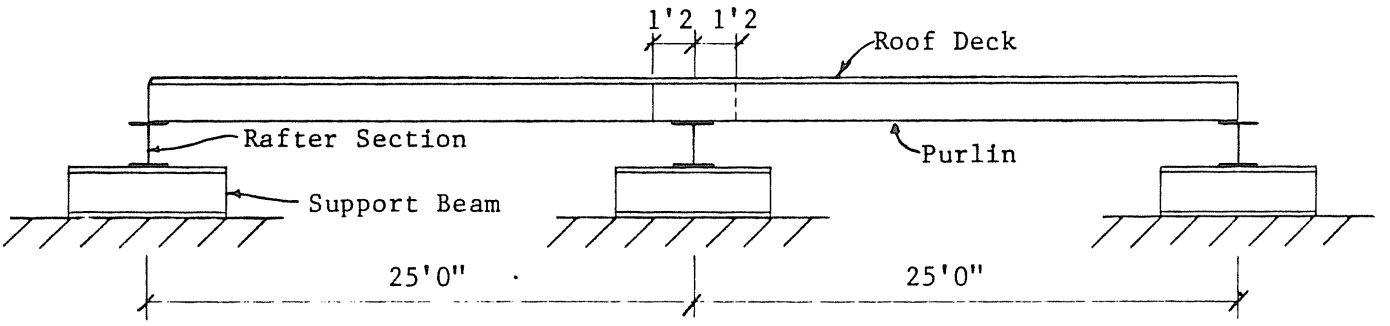

a) Elevation

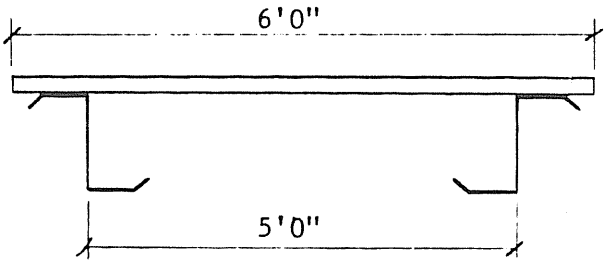

b) Section

Figure 1. Two Span Test Configuration

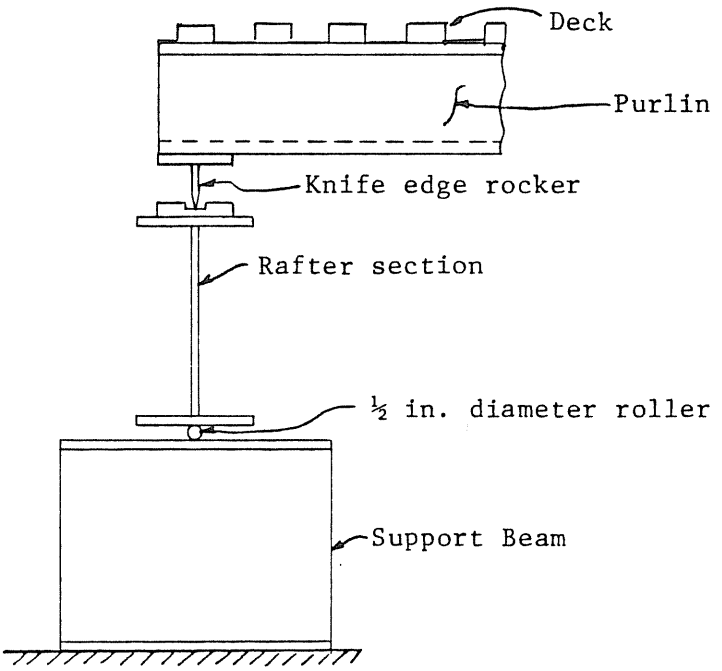

Figure 2. Support Rocker Details

made. A rocker, as shown in Figure 2, was placed between the purlin and the rafter section and a roller was placed between all but one rafter section and set of support beams.

Instrumentation consisted of strain gages on the lower lip and flange, oriented parallel to the purlin centerline and located immediately outside the lap, horizontal and vertical strain gages on the lower portion of the web, and vertical deflection gages (dial gages) at the midspan of each purlin. For one test, strain gages were also located at the centerline of one span.

Before testing, cross-sectional dimensions at each end of each purlin were measured using a protractor, metal scale and micrometer. The dimensions were averaged and cross-sectional properties required for the analysis procedures were calculated. After testing a tensile coupon was cut from the first purlin to fail and the yield stress was determined using the 0.2% offset method. The data is summarized in Table 1.

Load was applied to the system using 3 in. by 8 in. by 16 in. solid concrete blocks weighing 33.0 lbs. each. The blocks were set directly in the troughs of the roof deck at approximately 1 ft. on center. For each test, the purlin-deck system was first loaded to the working load, determined using the proposed analysis procedure and AISI allowable stresses (1,2), unloaded, and then loaded to failure. The concrete blocks were placed on the deck maintaining symmetry with respect to the longitudinal axis and approximately uniform load along the purlin. Load increments were initially 33 psf and were decreased to 4.25 psf near failure.

After each load increment, strain gage and deflection data were recorded. This information was used to develop load-deflection and load-stress relationships and stress distributions over cross sections. The resulting relationships were then compared to theoretically developed curves. The theoretical load-

TABLE 1

TEST PURLIN DIMENSIONS AND PROPERTIES

Dimension or Property	Test Number				
	2-1	2-2	2-3	3-1	3-2
Depth, in.	8.00	8.00	8.00	8.00	8.00
Flange Width, in.	3.08	3.00	3.00	2.98	2.90
Lip Length, in.	0.83	0.70	0.70	0.69	0.65
Thickness, in.	0.079	0.066	0.066	0.066	0.067
Lip Angle, deg.	42.0	39.5	39.5	40.7	38.5
$\overline{X}$, in.	0.4739	0.4215	0.4215	0.4172	0.4012
$\overline{Y}$, in.	0.0138	0.0730	0.0730	0.0686	0.0505
I_{xxt}, in.^{4}	12.91	10.18	10.18	10.13	10.13
I_{yyt}, in.^{4}	1.234	0.871	0.871	0.851	0.792
I_{xyt}, in.^{4}	2.306	1.679	1.679	1.655	1.595
I_{xyb}, in.^{4}	1.543	1.151	1.151	1.137	1.106
Yield Stress, ksi	65.2	75.2	75.2	66.8	61.3

deflection relationship at each dial gage location in each test was predicted using a standard stiffness procedure with an effective moment of inertia to account for out-of-plane bending. Calculation of this effective moment of inertia is described later in this report.

COMPARISON OF EXPERIMENTALS RESULTS WITH ANALYTICAL PREDICTIONS

Comparisons of experimental and analytical results for the five tests are described in this section. The two span tests are identified as 2-1, 2-2, and 2-3, and the three span tests as 3-1 and 3-2.

Test 2-1

A summary of experimental and analytical data for this two-span test is found in Appendix A. Failure was caused by web buckling immediately outside of the lap in one purlin. The failure load was 190 plf/purlin compared with a predicted load of 141 plf/purlin. This load was calculated using the method described in Reference 1 and the section properties shown in Figure A.1.

The experimentally determined load-deflection relationships, measured at the midspan of each purlin, are shown in Figure A.2, together with the predicted relationship.

Strain gages were glued to one purlin immediately adjacent to the lap and located as shown in Figure A.1. The strain data was converted to stress using Hook's Law for plane stress and plotted as shown in Figure A.3. The load-stress relationship is linear until near failure indicating that slippage in the lap connection did not occur and that drift did not exist in the instrumentation system.

The predicted stress distribution over the cross-section for both pinned and fixed end conditions, together with the experimentally obtained stress for a load of 123.8 plf/purlin is shown in Figure A.4. The experimental stress level is between the two end condition levels indicating an undesired restraint in the test set up.

The predicted failure load is significantly lower than the measured failure load. The restraint in the purlin support system is believed to be the cause and modification, as described in the previous section, was made. Results of this test are not considered valid for purlins supported by building frames.

Test 2-2

A summary of experimental and analytical data for this two-span test is found in Appendix B. Failure was caused by web buckling immediately outside of the lap in one purlin. The failure load was 121 plf per purlin compared with a predicted load of 115 plf/purlin, a difference of 5.2%. The predicted load was calculated using the method described in Reference 1 and the section properties shown in Figure B.1

The experimentally determined load-deflection relationships, measured at the mid-span of each purlin, are shown in Figure B.2 together with the predicted relationship. The effective moment of inertia, described in the next section was used for the calculations. Excellent agreement was obtained.

Strain gages were glued to one purlin immediately adjacent to the lap and located as shown in Figure B.1. The recorded strain data was converted to stress and is plotted versus load in Figure E.3. The load-stress relationship is linear until failure indicating that slippage in the lap connection did not occur nor was there drift in the data aquisition system.

Comparison of the predicted and experimentally obtained stress distributions at the strain gaged cross section are shown in Figure B.4. Only fair agreement was obtained.

It is apparent from the developed data that the proposed method accurately predicts deflections and failure load but is only a fair approximation of the stress distribution at the critical section.

Test 2-3

A summary of experimental and analytical data for this two-span test is found in Appendix C. Failure was caused by local buckling in both the compression flange and the web immediately outside of the lap of one purlin at a load of 120 plf/purlin. The predicted failure load of 115 plf per purlin was calculated using the proposed method and the section properties shown in Figure C.1. This load is 5.2% below the experimental failure load.

The experimentally determined load-deflection relationships, measured at the mid-span of each purlin, are shown in Figure C.2. together with the predicted relationships. Excellent agreement was obtained.

Strain gages were not used in this test.

The proposed method accurately predicted the failure load and the load-deflection relationship.

Test 3-1

A summary of experimental and analytical data for this three span test is found in Appendix D. Failure was caused by local buckling of the lip and compression flange in the positive moment region of the two end spans. The failure load was 153 plf/purlin compared with a predicted load of 144 plf/purlin. However, this predicted load was based on a combined shear-bending induced web buckling immediately adjacent to the end of the lap in the exterior spans.

The load was calculated using the method described in Reference 1 and the section properties shown in Figure D.1.

The experimentally determined load-deflection relationships, measured at the point of maximum deflection in the exterior spans, are shown in Figure D.2 together with the predicted relationship. The agreement for one purlin line was excellent. No explaination was found for the disagreement in the other purlin line.

Strain gages were glued to one purlin immediately adjacent to the lap end of the exterior span and located as shown in Figure D.1. The strain data was converted to stress using Hook's law and plotted as shown in Figure D.3. Nonlinearity was due either to gage creep or premature local buckling at the midspan of the exterior span. If local buckling did occur, the effective moment of inertia is reduced at midspan, thus increasing the moment and stress in the negative moment regions. Wrinkling or local buckling of the compression flange in the exterior spans was observed before the failure load was reached.

The predicted and experimental stress distributions at the gaged cross-section, for a load of 66 plf/purlin, is shown in Figure D.4. The experimental stress level is considerably lower than that predicted by the proposed method. It is felt that this discrepancy was due to the ignored rotational restraint of the deck or to gage creep.

The proposed method accurately predicted the load-deflection relationship. Since the failure mode was not in agreement with the assumed failure mode of Reference 1, no statement can be made concerning the accuracy of prediction of the failure load. From the lack of agreement in the stress distributions, it is felt that a reexamination of the assumption regarding torsional restraint of the deck is necessary.

Test 3-2

A summary of experimental and analytical data for this three span test is found in Appendix E. Failure was caused by web crippling at an end bearing location (exterior rafter support of exterior span). The failure load was 143 plf/purlin. Continued loading caused a similar bearing failure at a location diagonally opposite to the first failure at a load of 148 plf/purlin. Before failure, significant local buckling of the upper flanges of the exterior purlins was observed in regions of positive bending moment. The predicted failure load was 152 plf/purlin based on an assumed failure load of web buckling immediately outside of the lap in the exterior span. This failure load coincided well with the experimental failure load, however, the predicted failure mode was from web buckling rather than the actual failure mode of web crippling. Prior to failure, wrinkling or buckling was observed in the compression flange in the positive moment region. It was noted that the stiffener lip for this compression flange did not meet the minimum edge stiffener requirements of the AISI specification.

The experimentally determined load-deflection relationships, measured at the midspan of the outside purlins, are shown in Figure E.2 together with the predicted deflection. The predicted relationship is considered accurate.

Strain gages were glued to one exterior purlin at two cross-sections: immediately outside of the lap and at the midspan. Locations are shown in Figure E.1. The experimentally determined load-stress relationships are shown in Figure E.3. Nonlinearity in the curves was caused by premature local buckling or by drift in the strain gage data aquisition system.

Stress distributions at the two gage cross-sections were predicted using the proposed analytical technique and are plotted along with experimental values in Figures A.4 and A.5. Excellent agreement was obtained at the lap

location, however, the predicted distribution at mid-span is not in agreement with the measured stresses. The discrepency was caused by rotational restrain of the deck which was neglected in the development of the proposed analysis technique.

It is apparent from the test results that the proposed procedure accurately predicts the stress distribution at the lap location. It is also apparent that the torsional restraint of the deck must be considered in computing the stress distributions at midspan e.g. in the positive moment region. It was also shown that the edge stiffeners are critical components of the purlin cross-section.

MODIFICATION OF ANALYSIS PROCEDURE

Analytical Modifications

When the top flange of a Z-purlin is restrained from lateral movement, the lower flange tends to deflect as shown in Figures 3a and 3b. Restraint of this movement comes from the torsional stiffness of the deck and deck-to-purlin connection and from the out-of-plane bending stiffness of the web. The analysis procedure in Reference 1 ignores this restraint, Figure 3c, which results in a significant over-estimate of the maximum stress in the flange as was discussed in the previous section. To account for the restraint effect, the previous procedure is modified to include an elastic spring in the plane of the lower flange as shown in Figure 3d. The out-of-plane analysis required in the proposed procedure is then a beam on the elastic foundation with spring stiffness K.

The equivalent lateral spring stiffness of the web alone can easily be determined from

$$K = \frac{F}{\Delta} \tag{2}$$

where Δ and F are as shown in Figure 4a and

$$\Delta = \frac{Fh^3}{3D}$$

with

$$D = \frac{Et^3}{12(1-u^2)}$$

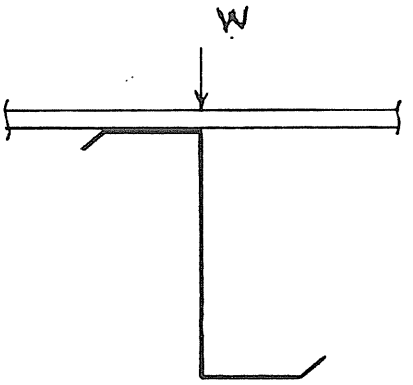

a) Original Position

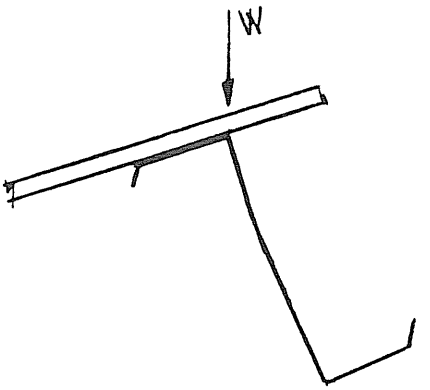

b) Deflected Position

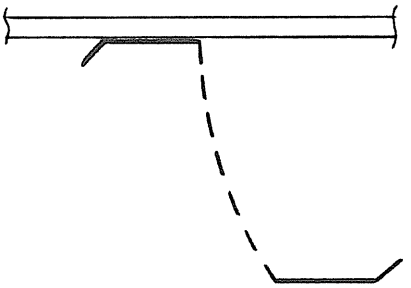

c) Simplifying Assumption
(Reference 1)

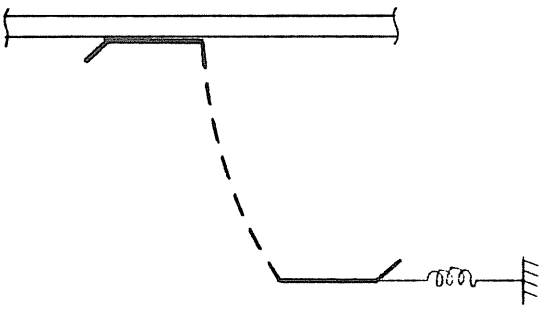

d) Modification
(Present Analysis)

Figure 3. Deflected Position of Partially Restrained Z-Purlin Section

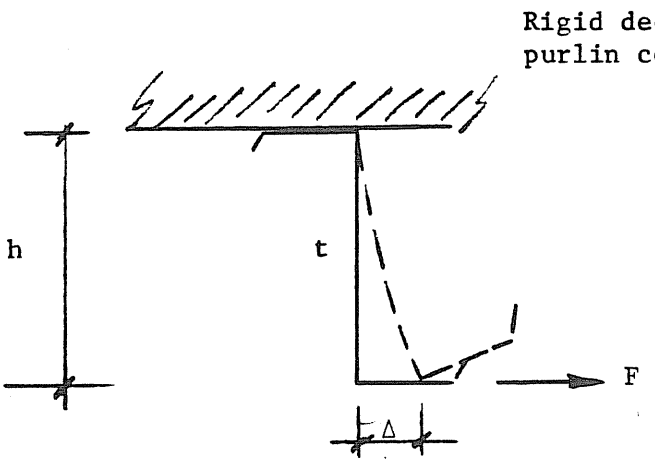

a) Lateral Web Stiffness

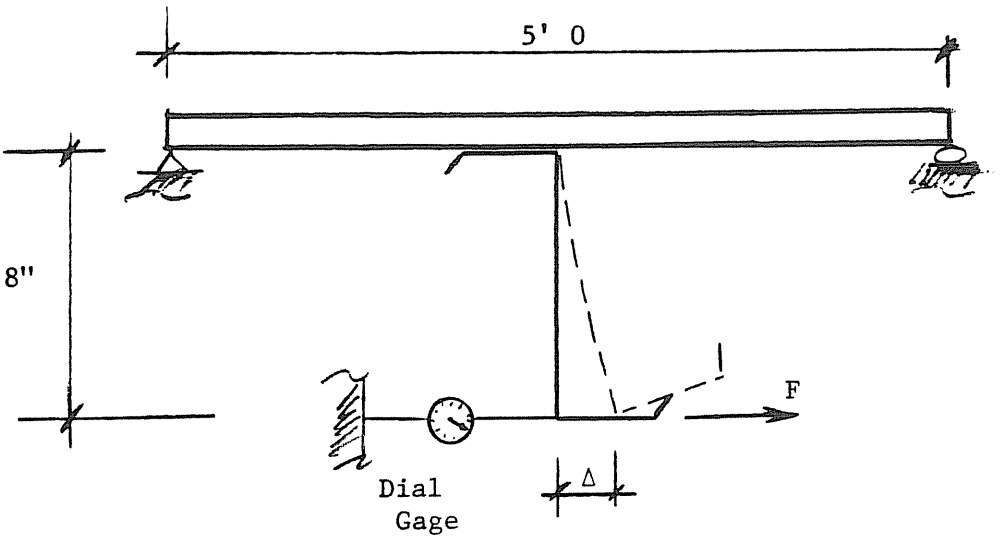

b) Experimental Determination of Lateral Stiffness

Figure 4. Lateral Restraint of Free Flange

where D = the plate rigidity, h = the web depth, t = web thickness, E = modulus of elasticity, and u = Possion's ratio. Hence

$$K = \frac{3D}{h^3} \tag{3}$$

The torsional restraint of the complete roof system, deck, connection and purlin, can only be determined experimentally. Figure 4b shows the experimental setup used to determine K for the deck-fastener-purlin combination of this study.

Once the equivalent lateral stiffness is known, the horizontal bending of the unrestrained flange is analyzed as previously, except a continuous lateral elastic foundation is added. All other parts of the analysis are identical.

Example Calculations

Example calculations follow for the standard 8 x 3 Z 0.064 three span purlin shown in Figure 5. Properties for the full, transformed and required partial sections are shown, respectively, in Figures 5b, 5c, and 5d. The lower flange restraint, assuming a perfectly rigid deck, is shown in Figure 5e. This rigidity is an upper limit and is used for these example calculations only. Deck flexibility should be included in design calculations.

1. Calculate ficticious horizontal load and effective I_h:

$$W_h' = W(I_{xyb} / I_{xx}) = 107(1.091/9.676)$$

$$= 12.0 \text{ lb/ft}$$

$$I_h' = (I_{xxt} I_{yyt} - I_{xyt}^2)/I_{xxt}$$

$$= ((9.696)(0.849) - 1.592^2) / 9.696 = 0.5876 \text{ in.}^4$$

2. Analyze for horizontal bending using a stiffness analysis.

   For this example, the program STRUDL was used. The model is shown in Figure 5f and the output is found in Appendix F. The horizontal moment in the lower flange immediately outside the lap in the exterior span was found to be:

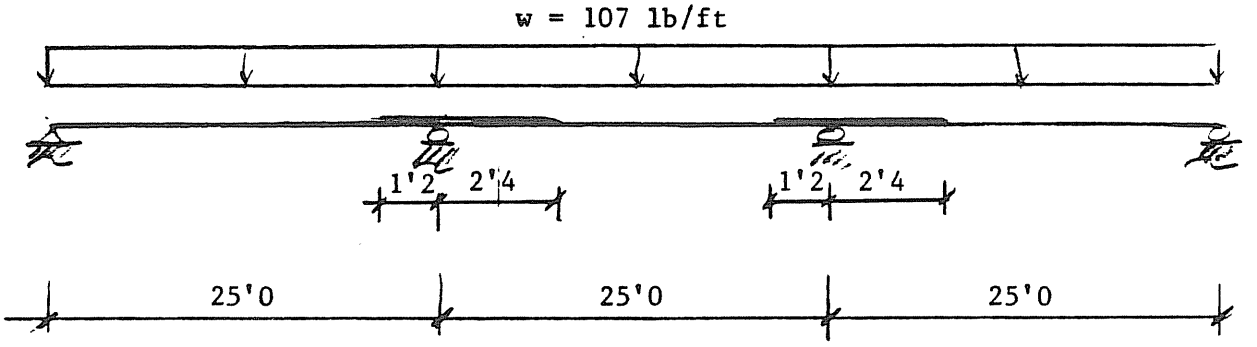

a) Spans and Lap Lengths

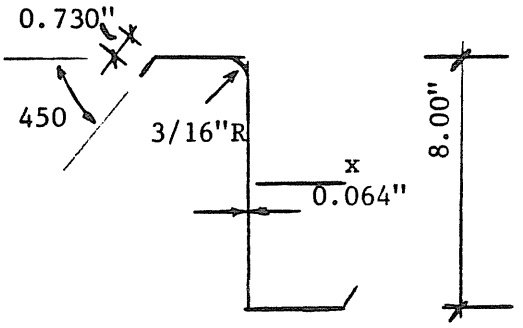

I_{xx} = 10.185 in^4
I_{yy} = 2.146 in^4
I_{xy} = 3.441 in^4

b) Full Section

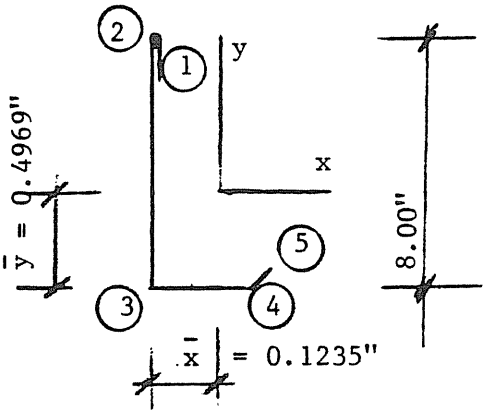

I_{xxt} = 9.696 in^4
I_{yyt} = 0.849 in^4
I_{xyt} = 1.592 in^4

c) Transformed Section

Figure 5. Dimensions and Properties for Example Calculations

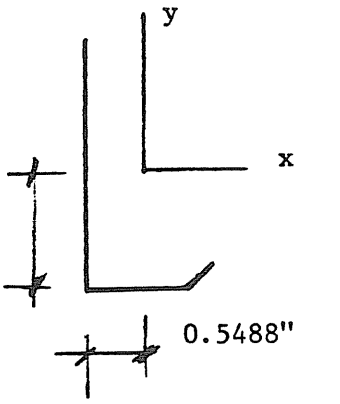

$I_{xyb} = 1.091 \text{ in}^4$

d) Web and Lower Flange

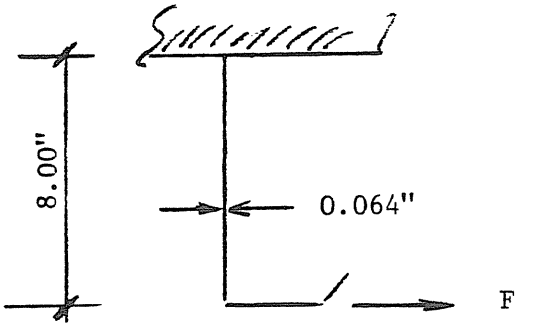

$$D = \frac{(29{,}500)(0.064)^3}{12(1-0.3^2)} = 0.708$$

$$K = \frac{3\ (0.708)}{(8.0)^3} = 0.00415 \text{ k/"/"}$$

$$= 49.8 \text{ lb/in/ft}$$

e) Lateral Stiffness

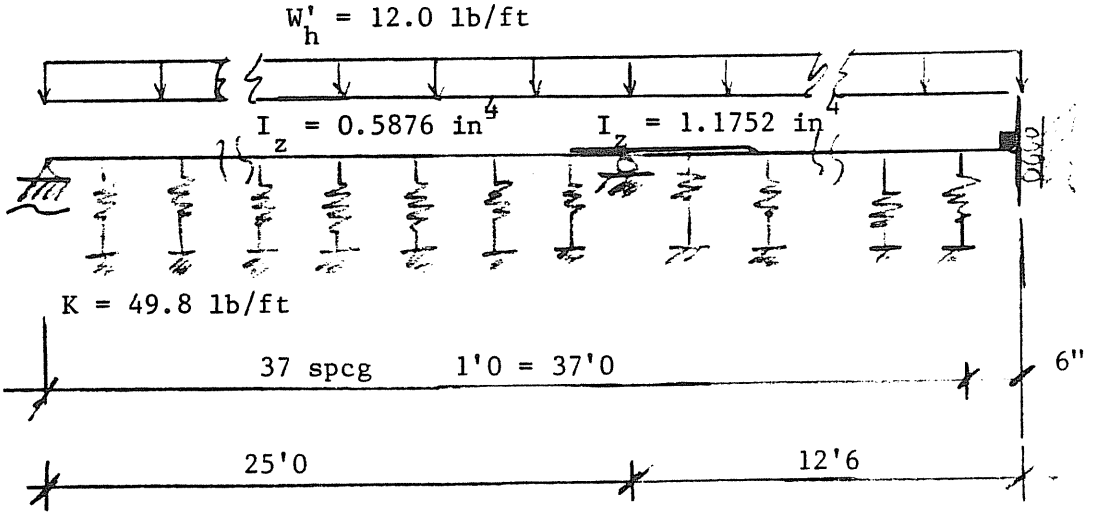

f) Lower flange analysis model

Figure 5. Dimensions and Properties for Example Calculations Continued

$M_h = 1.707$ in-kips

3. Analyze for real vertical bending moments using a stiffness analysis.

Again the program STRUDL was used. The model is shown in Figure 5a and the moment and shear in the section immediately outside the lap in the exterior span were found to be:

$M'_v = 64.28$ in-kips $\qquad V'_v = 1.500$ k

4. Determine ficticious vertical moment from ficticious horizontal moment.

$$M''_v = M_h I_{xyt} / (I_{xxt} I_{yyt} - I_{xyt}^2)$$

$$= (1.712)(1.592) / ((9.696)(0.849) - 1.592^2)$$

$$= 0.478 \text{ in-kips}$$

5. Add real and ficticious vertical moments.

$$M_v = M'_v + M''_v = 64.28 + 0.478$$

$$= 64.8 \text{ in-kips}$$

6. Calculate stresses at the critical section (outside of lap, exterior span) using Equation 2.13 of Reference 1.

$$\sigma = \frac{M_v y_t}{I_{xxt}} - \frac{M_h I_{xxt} x_t}{I_{xxt} I_{yyt} - I_{xyt}^2}$$

$$= \frac{64.8\, Y_t}{9.696} - \frac{(1.707)(9.696) x_t}{(9.696)(0.849) - (1.592)^2}$$

$$= 6.68\, y_t - 2.905\, x_t$$

7. Calculate stresses at corners of critical cross-section. Locations are shown in Figure 3c.

Normal stresses

Location	x, in.	y, in.	σ, ksi
1	0.4969	3.360	21.0 T
2	0.4969	3.877	24.5 T
3	0.4969	-4.124	29.0 C
4	-2.503	-4.124	20.3 C
5	-3.019	-3.607	15.3 C

Shear stresses in web

$\tau = V/dt = 1.50/(8.00)(0.064)$

$= 2.93$ ksi

8. Calculate allowable bending and shear stresses for web using AISI requirements. $F_y = 55.0$ ksi

$$\frac{h}{t} = \frac{8.00 - 2(0.064)}{0.064} = 123 > \frac{547}{\sqrt{55}} = 73.8$$

$F_v = 83{,}200/(123)^2 = 5.50$ ksi

$F_{bw} = 520{,}000/(123)^2 = 34.37$ ksi $0.6(55) = 33$ ksi

$F_{bw} = 33.0$ ksi

9. Compare actual stresses to allowable stresses.

a. Yielding

$f_{bw} = 29.0$ ksi < 33.0 ksi O.K.

b. Web Shear

$f_v = 2.93$ ksi < 5.50 ksi O.K.

c. Web buckling due to combined bending and shear

$(f_v/F_v)^2 + (f_{bw}/F_{bw})^2 \leq 1.0$

$(2.93/5.5)^2 + (29.0/34.37)^2 \leq 1.0$

$0.28 + 0.71 = 0.99 \leq 1.0$ O.K.

Section is satisfactory.

The calculations above are for a location immediately outside the lap. Similar calculations can be made for any location along the purlin.

Comparison with Experimental Data

The stress distributions predicted by the modified procedure at the exterior lap and midspan locations are compared to the experimental results for Test 3-2 in Figures 6 and 7, respectively. A lateral spring constant of $K = 17.6$ was used in the calculations. This constant was determined using the

experimental arrangement shown in Figure 4. A purlin section identical to that used in Test 3-2 with similar deck and identical fastener arrangement was used to experimentally determine K.

Figure 6 shows excellent agreement between the experimental and theoretical stress distributions at the lap location. Figure 7 shows good agreement for the lower half of the cross-section at the midspan location, however, the upper or compression flange predicted stresses are considerably lower than the measured stresses. During Test 3-2 premature wrinkling of the compression lip and flange in the positive moment region was observed because of an inadequate lip (see measured dimensions of purlins, Figure E.1). To investigate the possibility of increased stresses due to premature flange buckling, midspan section properties were recalculated assuming an effective flange width of 1.0 in. The resulting stress distribution is compared with the experimental results in Figure 8 and excellent agreement exists.

In test 3-1, failure was caused by local flange buckling at midspan of an exterior span at a load of 153 plf/purlin. Using the modified procedure with K = 17.6, the predicted failure load was 195 plf/purlin for a fully effective compression flange and 152 plf/purlin for a 1.0 in. effective compression flange width.

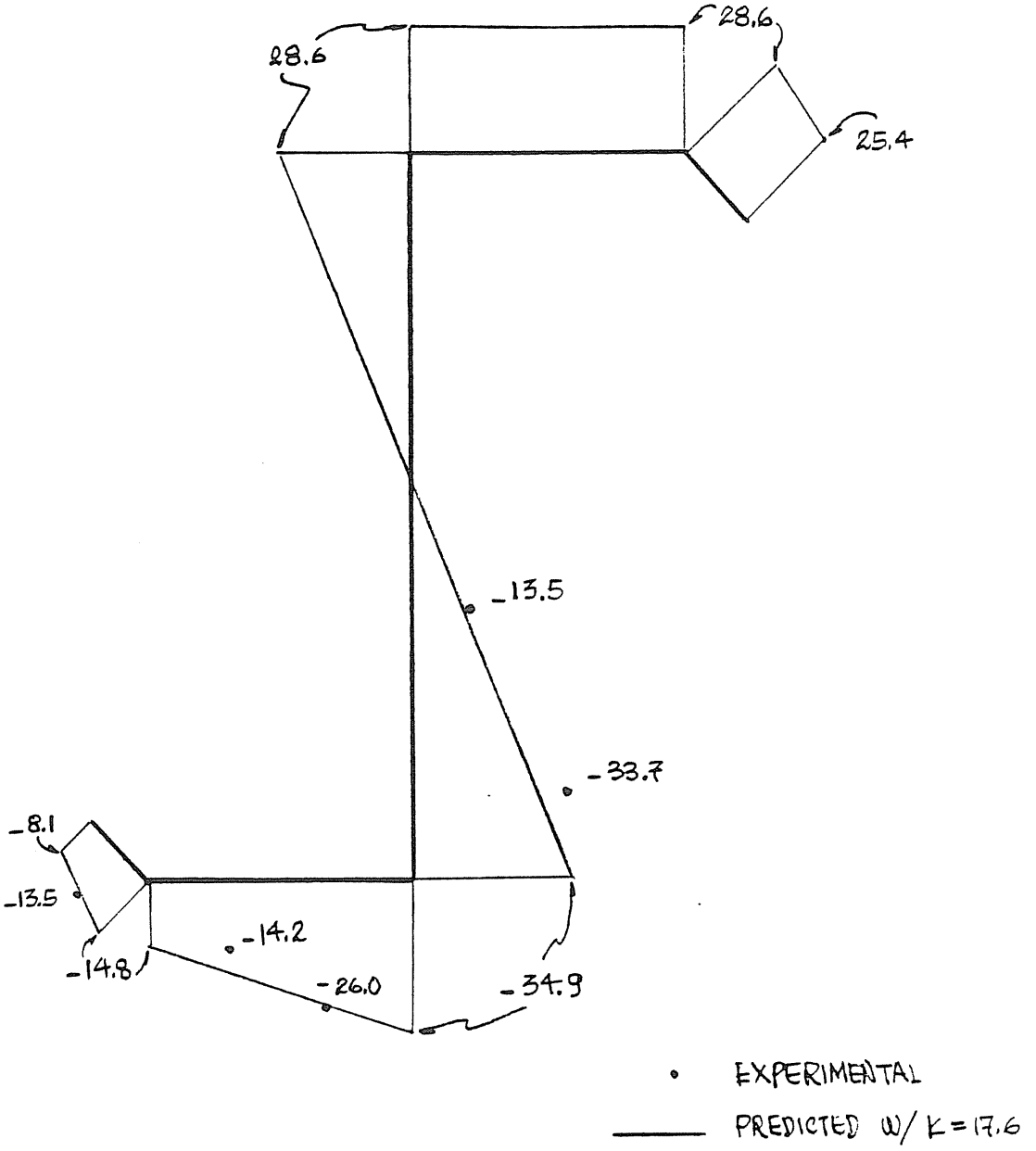

Figure 6. Experimental vs. Predicted Stress Distribution w/ Deck Restraint, Lap Location, Test 3-2

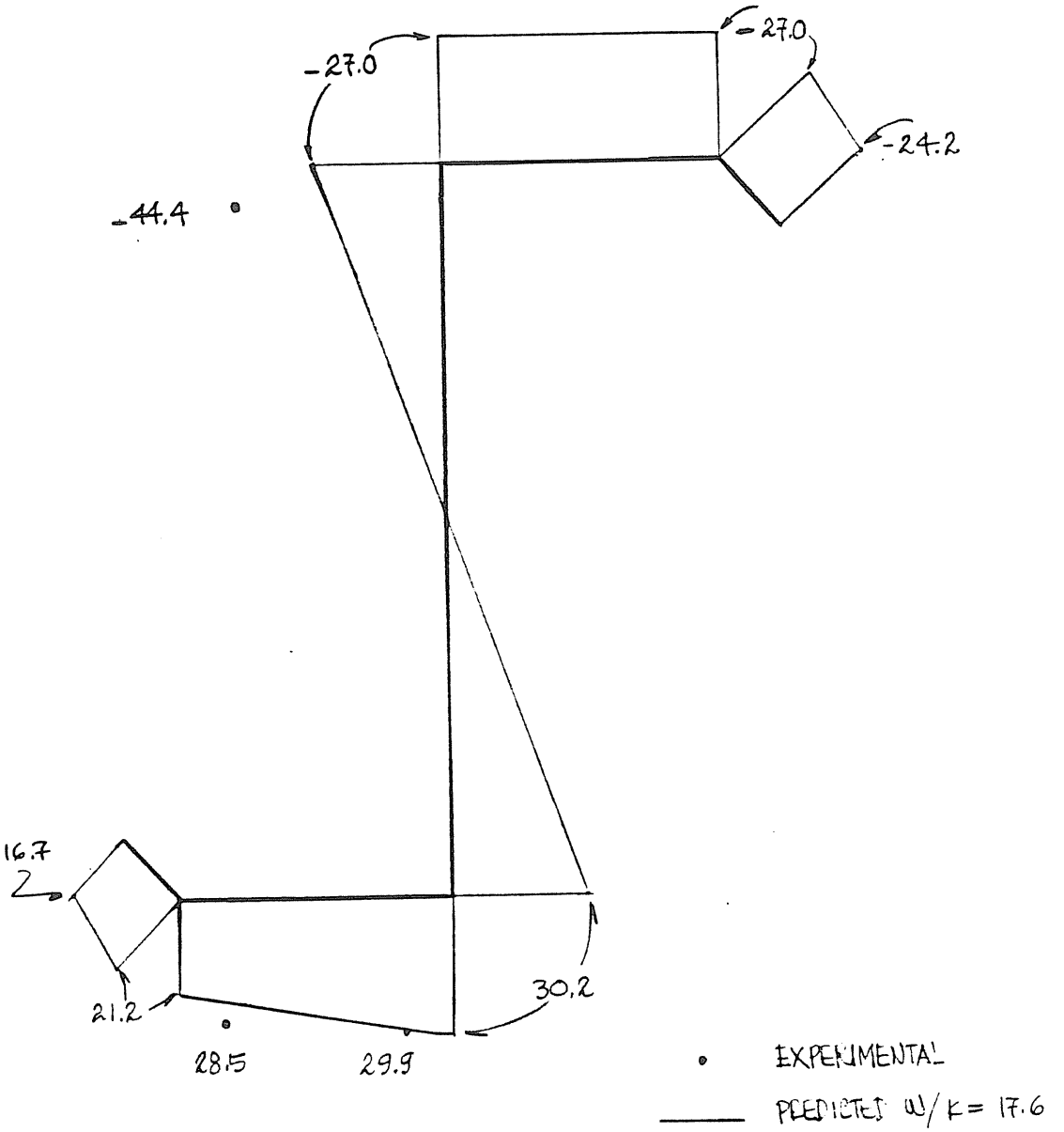

Figure 7. Experimental vs. Predicted Stress Distribution w/ Deck Restraint, Midspan Location, Test 3-2

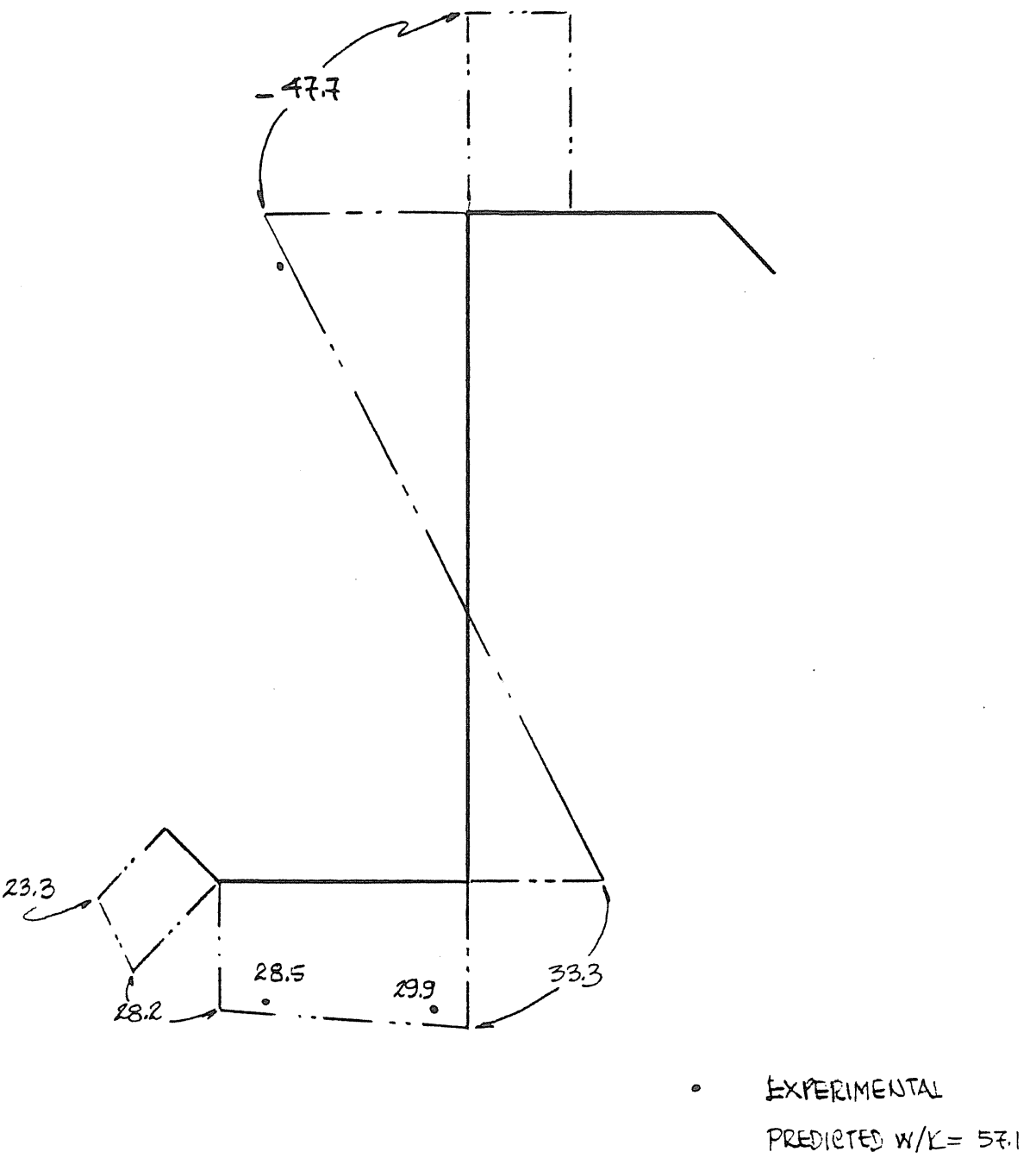

Figure 8. Experimental vs. Predicted Stress Distribution for 1 in. Effective Compression Flange Width, Midspan Location, Test 3-2

CONCLUSIONS AND RECOMMENDATIONS

Measured stress distribution found in tests of two span Z-purlin/deck systems were adequately predicted by the previously proposed analytical procedure with suggested modifications. Predicted failure loads using the stress distributions and AISI provisions were shown to be in good agreement with experimental results. The purlins used for the three span tests had inadequate stiffening lips which necessitated further modification of the proposed procedure. The final predicted results compared very well with measured stress distributions and failure loads.

It is recommended that the method be used for design. It is emphasized that adequate stiffening lips are required to develop the full strength of a purlin/deck system. It is noted that the equivalent lateral spring stiffness must be determined experimentally and that the values used in this report should not be applied generally. Insulation installed between the deck and the purlin can substantially affect the restraint of the deck.

Unfortunately, the method is somewhat cumbersome for routine design in that two stiffness analyses are required and one is an appoximation of a beam on an elastic foundation requiring substantial computer time. Additional analytical work might include the development of closed-form solutions for a flange supported by a continuous elastic spring.

The proposed procedure was developed for purlins with one flange continuously restrained by roof panels screwed to a purlin flange. The method can easily be modified for "floating" roof systems with lateral purlin support provided by

sag rods or straps at discrete locations.

The analytical and experimental work described here is strictly for gravity loading with the compression flange braced by roof panels in the positive moment region and the rafter providing lateral support at the location of maximum moment. Additional analytical and experimental study is required for safe application to uplift loading where the compression flange is substantially unbraced throughout the span.

REFERENCES

1. Wallace, B. J. and Murray, T. M., "Web Buckling of Continuous Lapped Z-Purlins," Progress Research Report submitted to Star Manufacturing Co., January, 1979.

2. "Specification for the Design of Cold-Formed Steel Structural Members, American Iron and Steel Instititute, New York, 1977.

APPENDIX A

Two Span Test 2-1

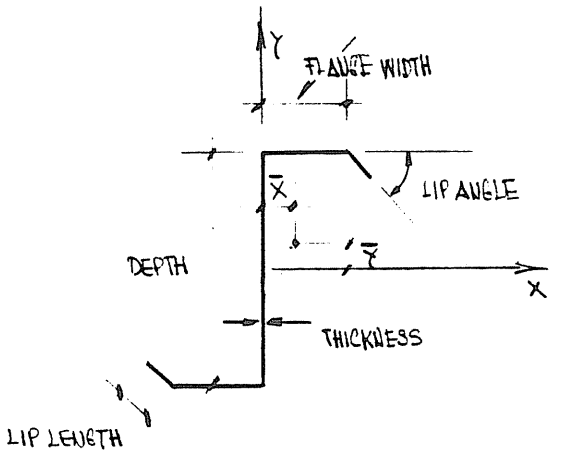

Dimension or Property	
Depth, in.	8.000
Flange Width, in.	3.080
Lip Length, in.	0.830
Thickness, in.	0.079
Lip Angle, deg.	42.00
$\bar{x}$, in.	0.474
$\bar{y}$, in.	0.014
Ixxt, in.^{4}	12.909
Iyyt, in.^{4}	1.234
Ixyt, in.^{4}	2.306
Ixyb, in.^{4}	1.543
Yield Stress, ksi	65.175

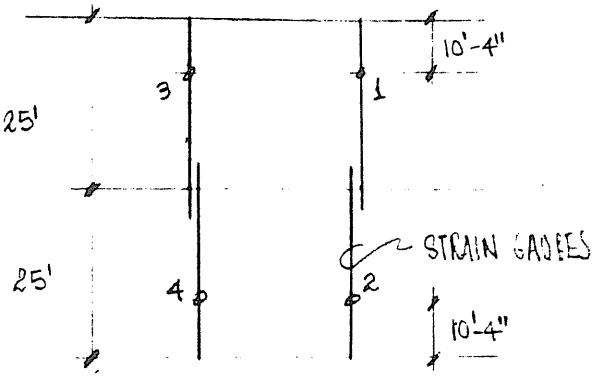

Dial Gauge Locaions

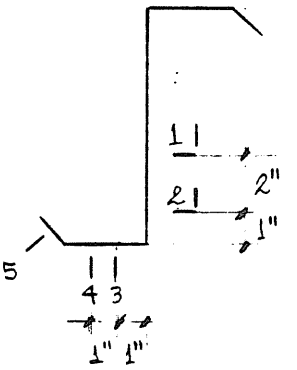

Strain Gauge Locations

Figure A.1 Section Properties and Instrumentation, Test 2-1

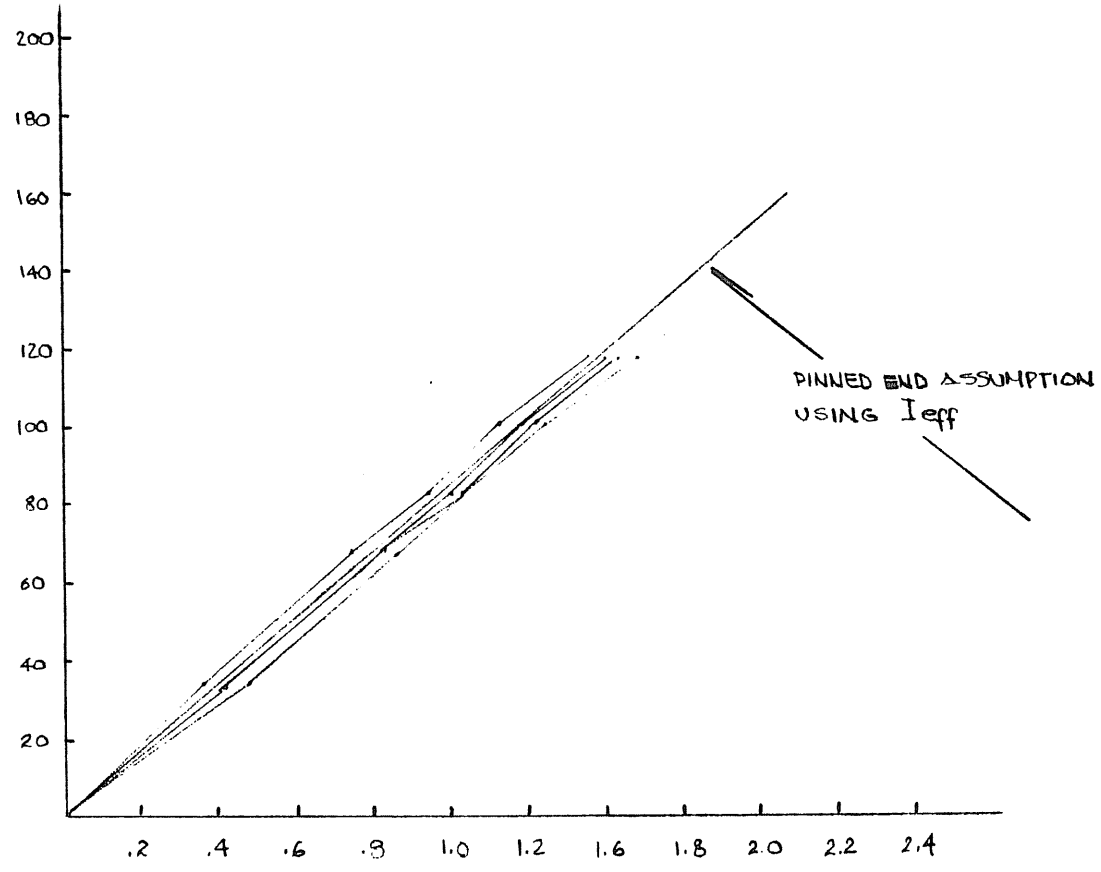

Figure A.2 Load vs. Midspan Deflections, Test 2-1

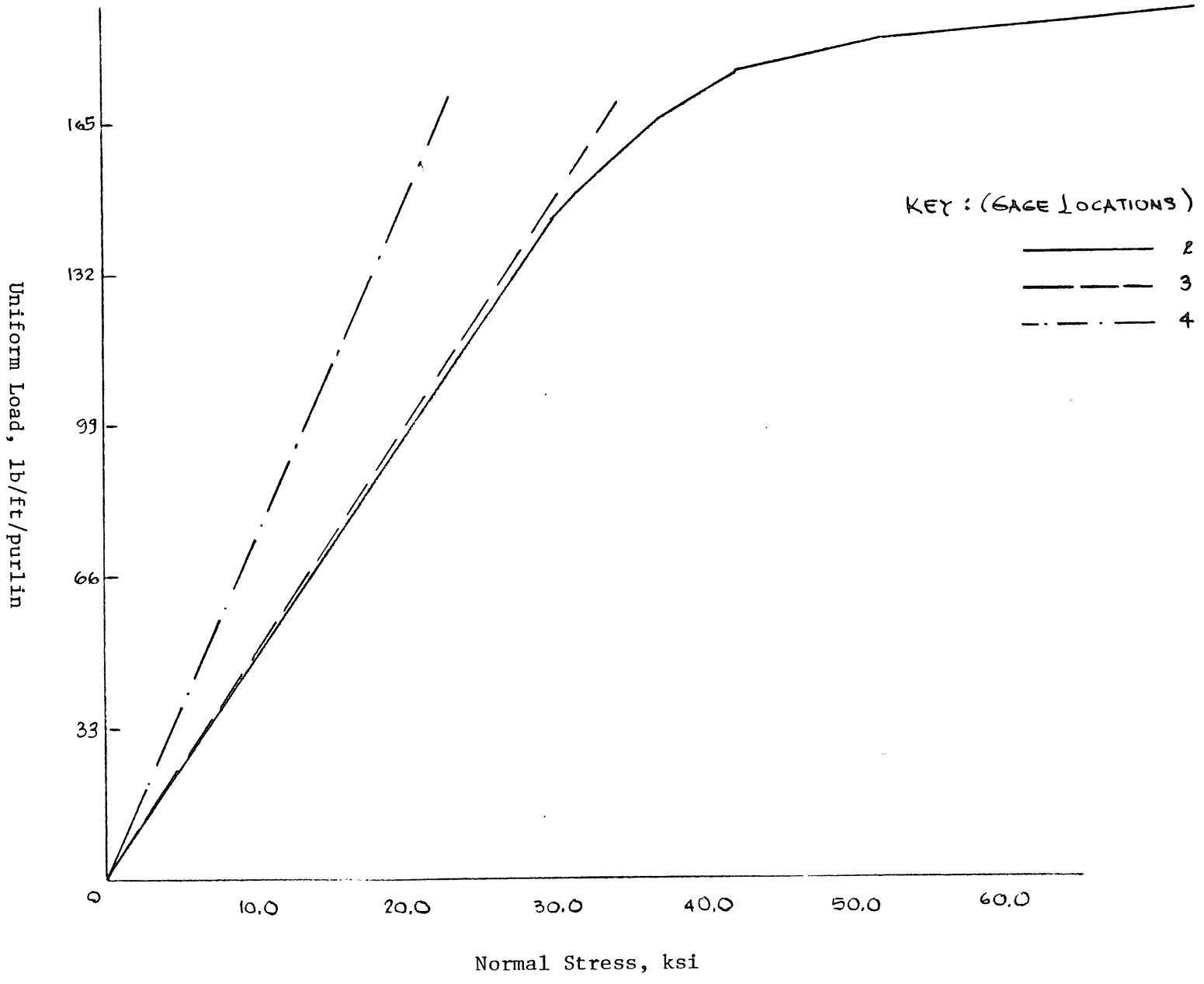

Figure A.3 Load vs. Normal Stress at Lap, Test 2-1

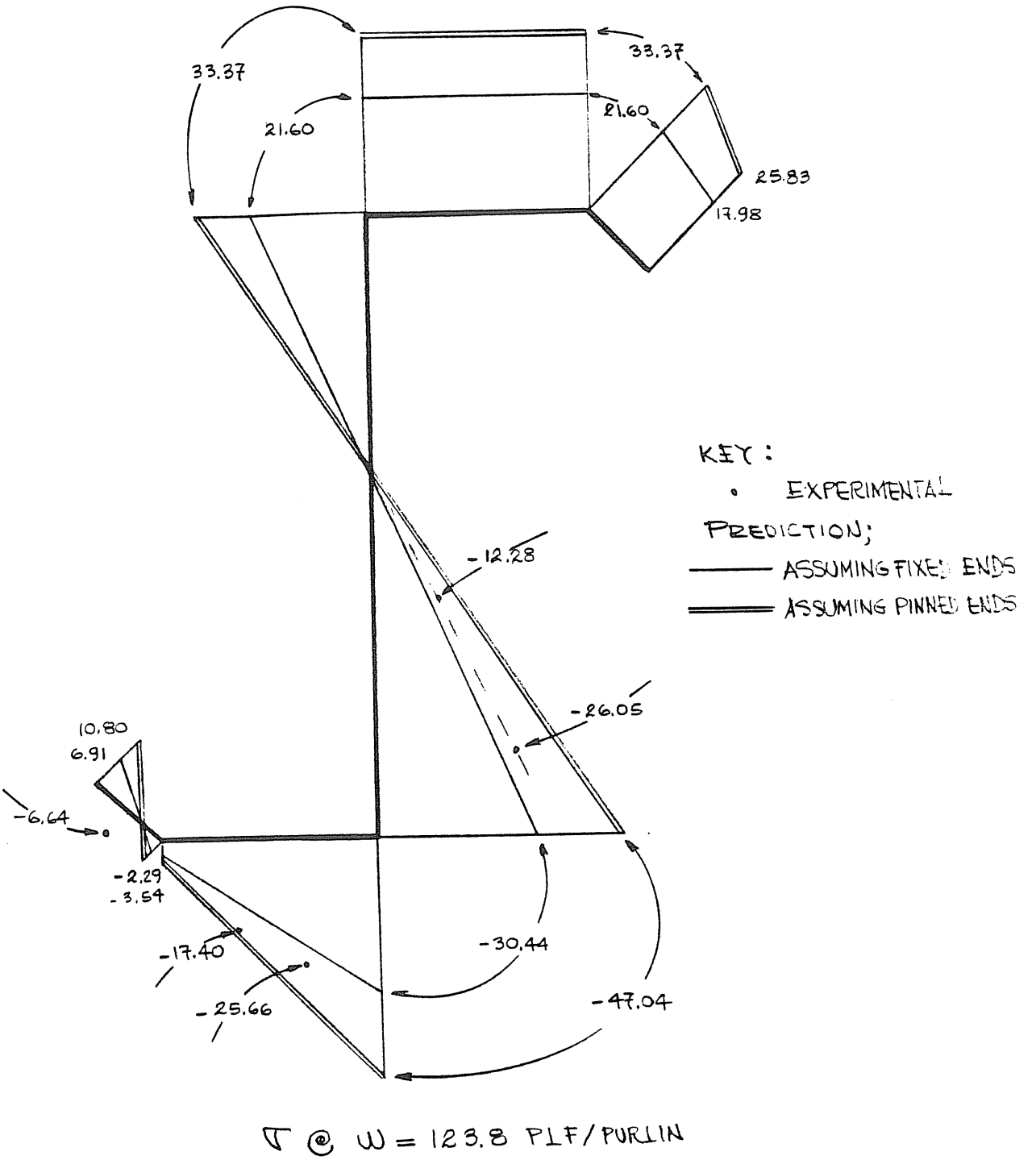

Figure A.4 Stress Distribution at Gaged Section, Test 2-1

APPENDIX B

Two Span Test 2-2

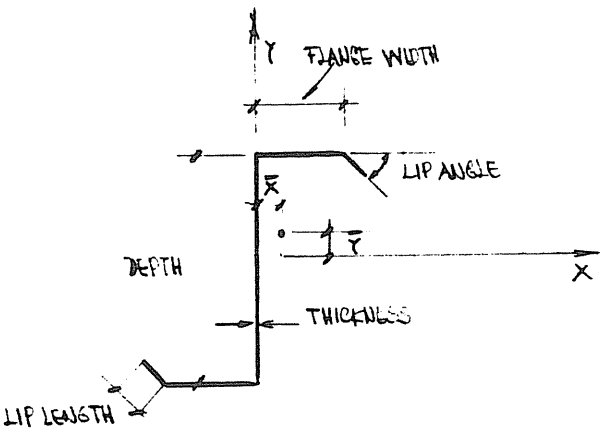

Dimension or Property	
Depth, in.	8.000
Flange Width, in.	3.000
Lip Length, in.	0.700
Thickness, in.	0.066
Lip Angle, deg.	39.50
$\bar{x}$, in.	0.422
$\bar{y}$, in.	0.073
Ixxt, $in.^4$	10.175
Iyyt, $in.^4$	0.871
Ixyt, $in.^4$	1.679
Ixyb, $in.^4$	1.151
Yield Stress, ksi	75.129

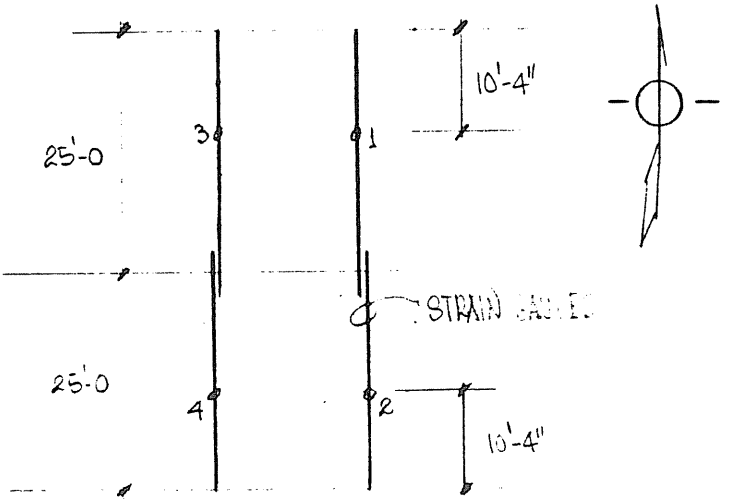

Dial Gauge Locations

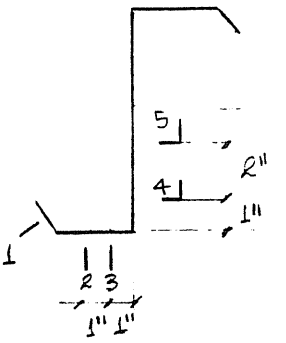

Strain Gauge Locations

Figure B.1 Section Properties and Instrumentation, Test 2-2

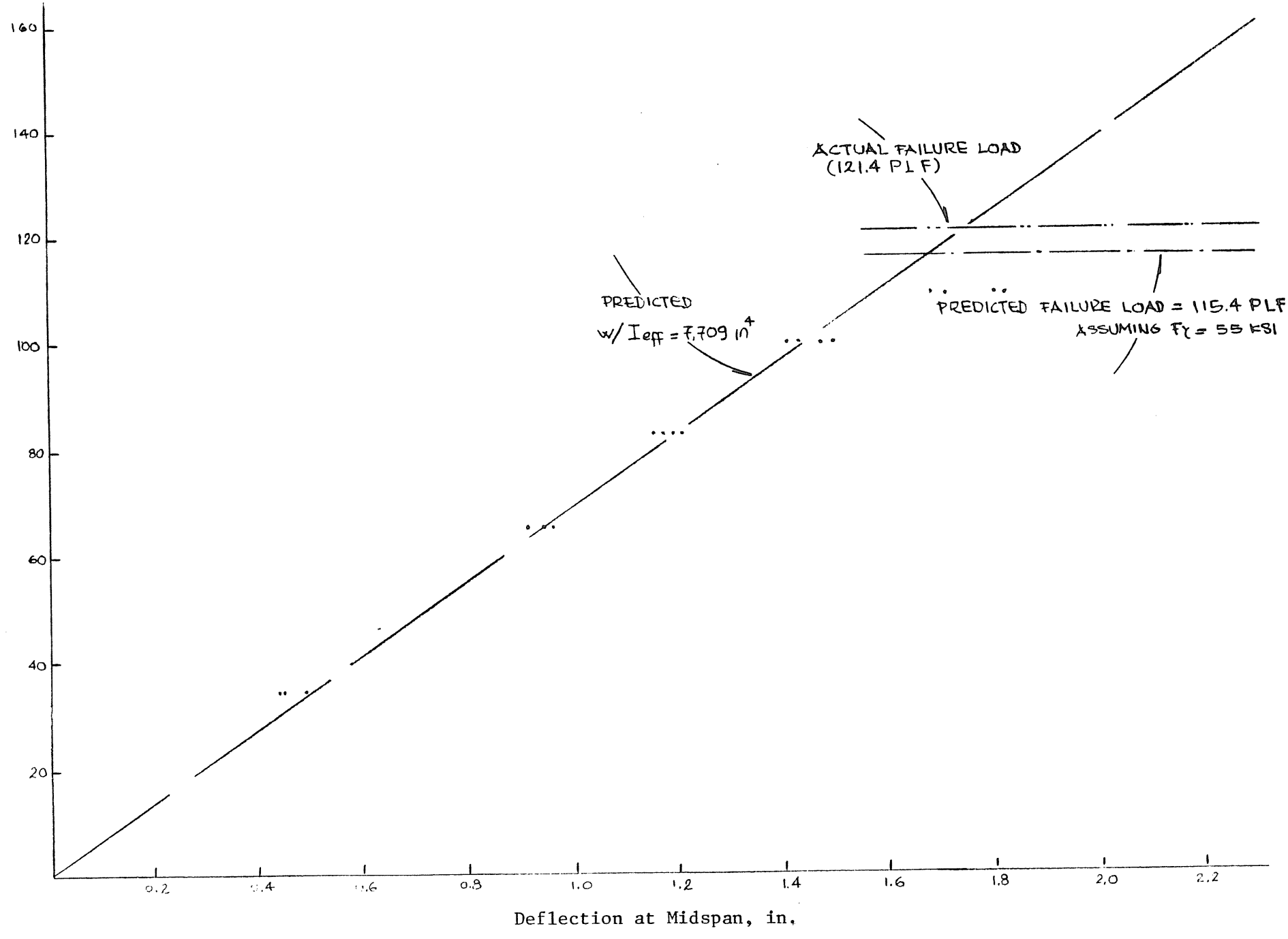

Figure B.2 Load vs. Midspan Deflections, Test 2-2

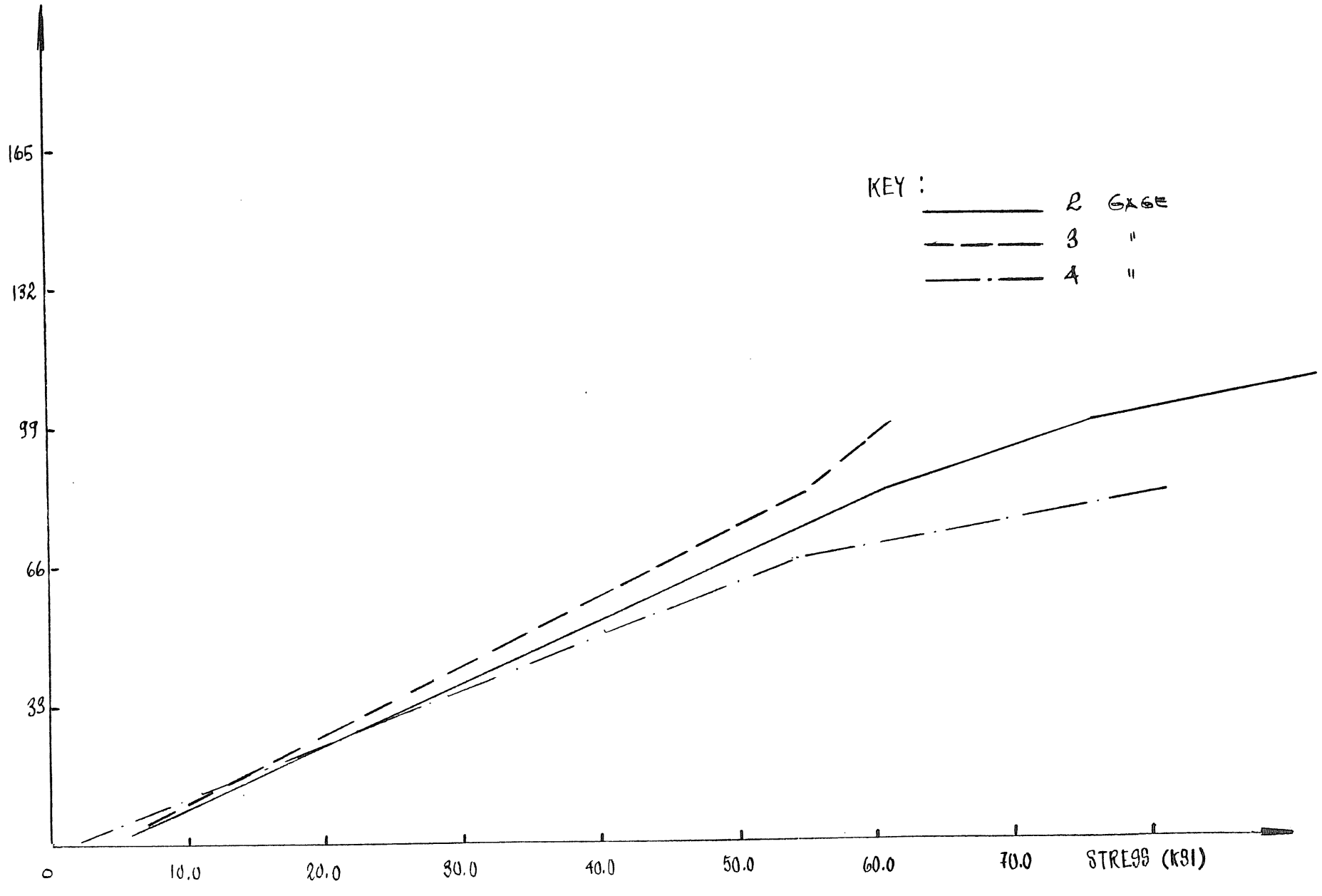

Figure B.3 Load vs. Normal Stress at Lap, Test 2-2

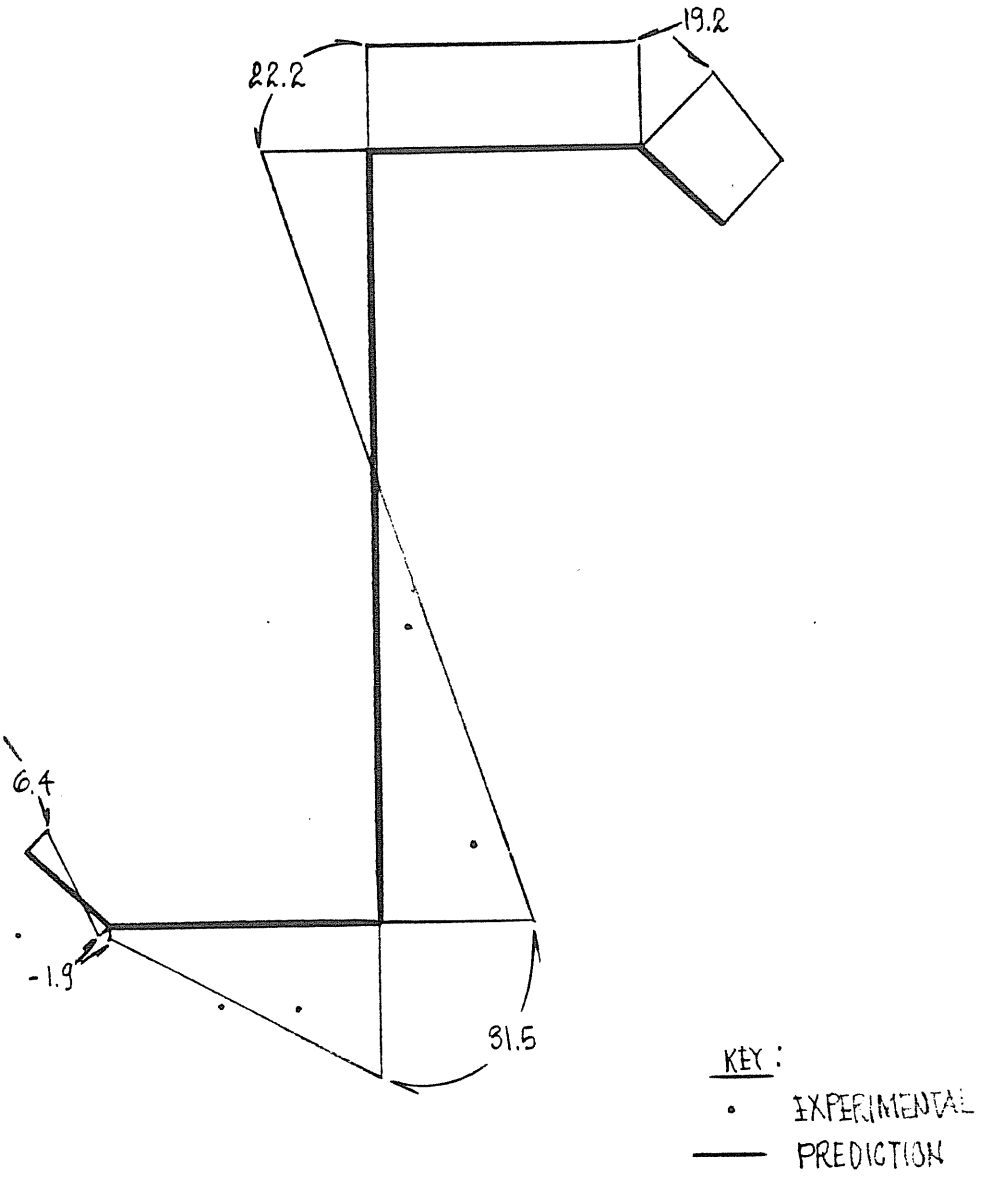

Figure B.4 Stress Distribution at Gaged Section, Test 2-2

APPENDIX C

Two Span Test 2-3

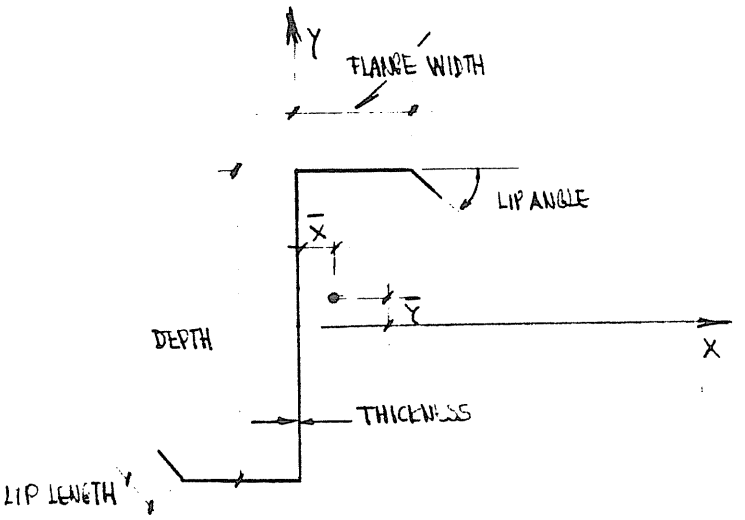

Dimension or Property	
Depth, in.	8.000
Flange Width, in.	3.000
Lip Length, in.	0.700
Thickness, in.	0.066
Lip Angle, deg.	39.500
$\bar{x}$, in.	0.422
$\bar{y}$, in.	0.073
Ixxt, in.^{4}	10.175
Iyyt, in.^{4}	0.871
Ixyt, in.^{4}	1.679
Ixyb, in.^{4}	1.151
Yield Stress, ksi	75.129

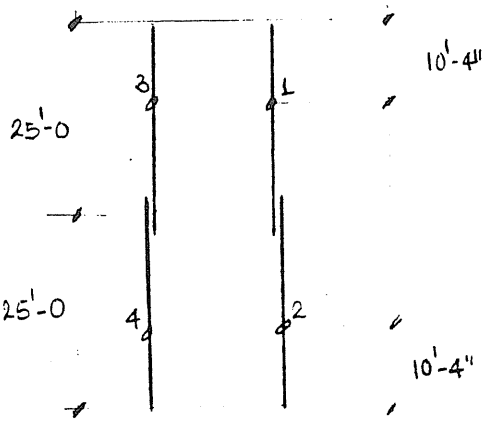

Dial Gauge Locations

Figure C.1 Section Properties and Instrumentation, Test 2-3

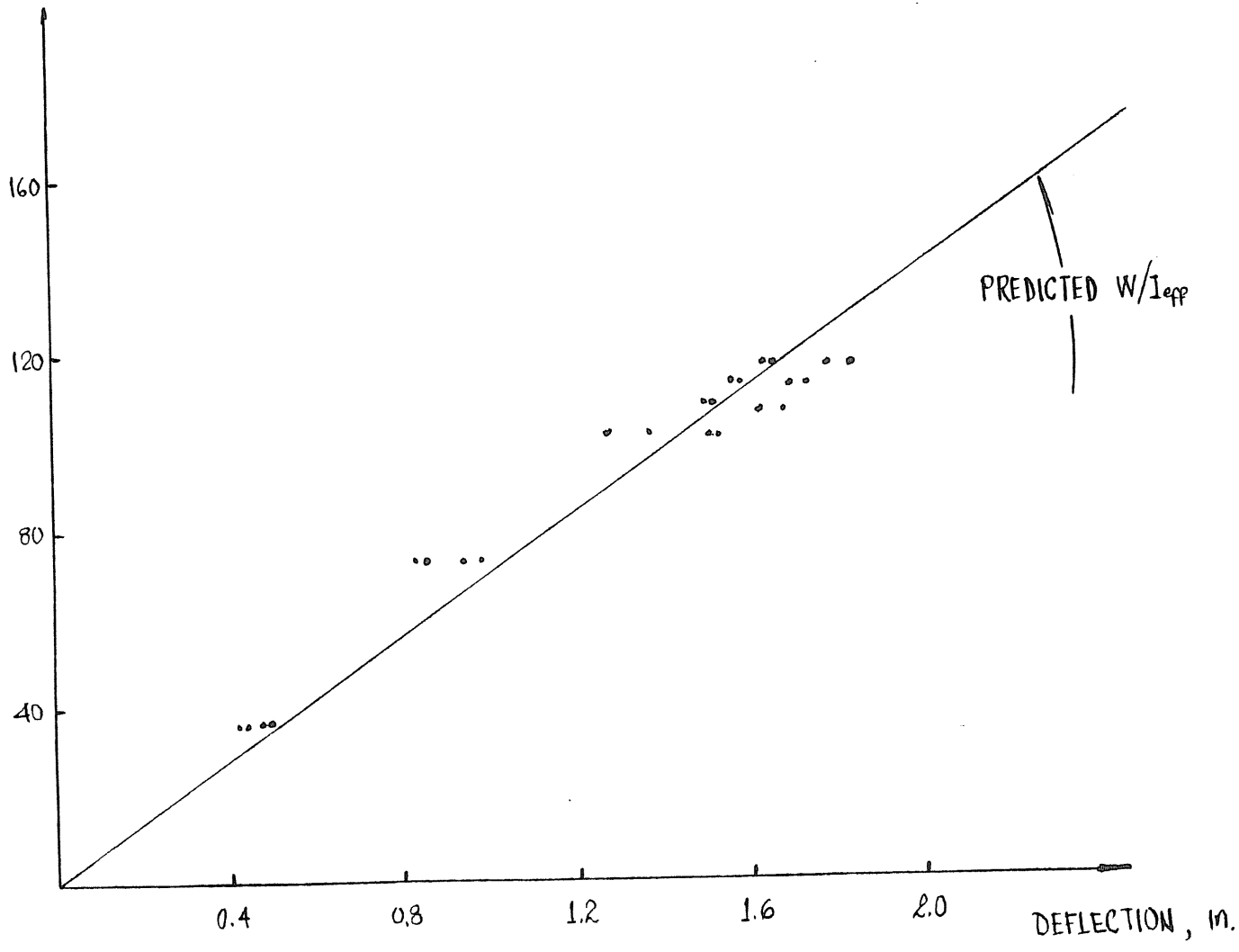

Figure C.2 Load vs. Midspan Deflections, Test 2-3

APPENDIX D

Test 3-1

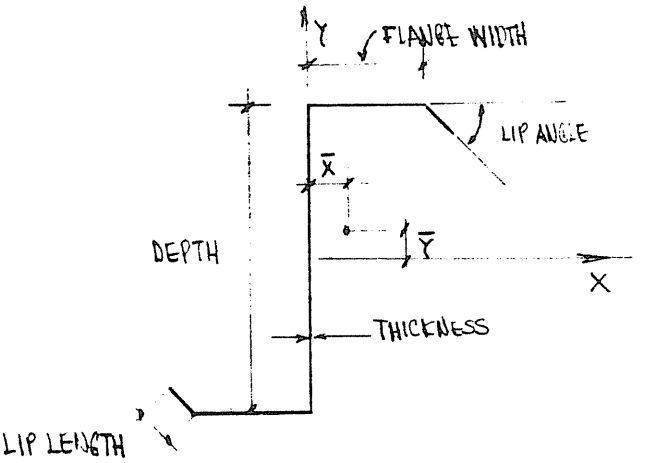

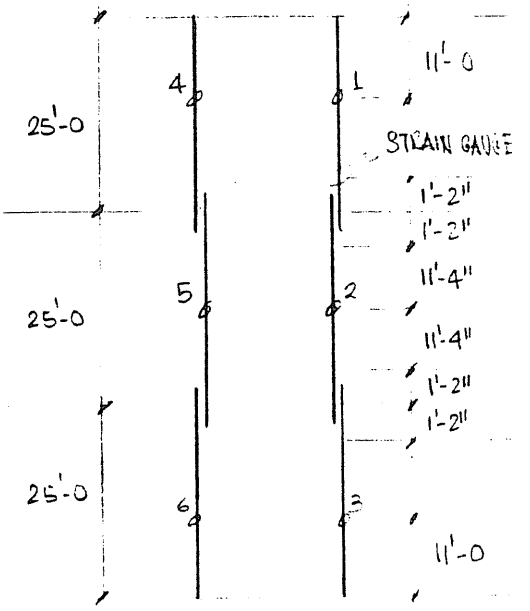

Dial Gauges Locations

Dimension or Property	
Depth, in.	8.000
Flange Width, in.	2.980
Lip Length, in.	0.690
Thickness, in.	0.066
Lip Angle, deg.	40.70
$\bar{x}$, in.	0.417
$\bar{y}$, in.	0.069
Ixxt, in.^{4}	10.132
Iyyt, in.^{4}	0.851
Ixyt, in.^{4}	1.655
Ixyb, in.^{4}	1.137
Yield Stress, ksi	66.835

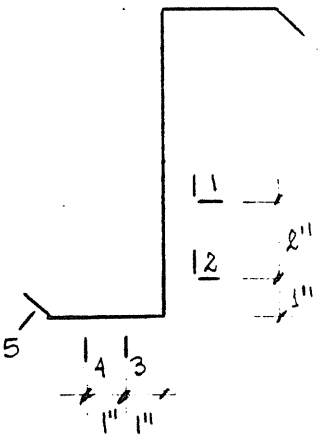

Strain Gauge Locations

Figure D.1 Section Properties and Instrumentation, Test 3-1

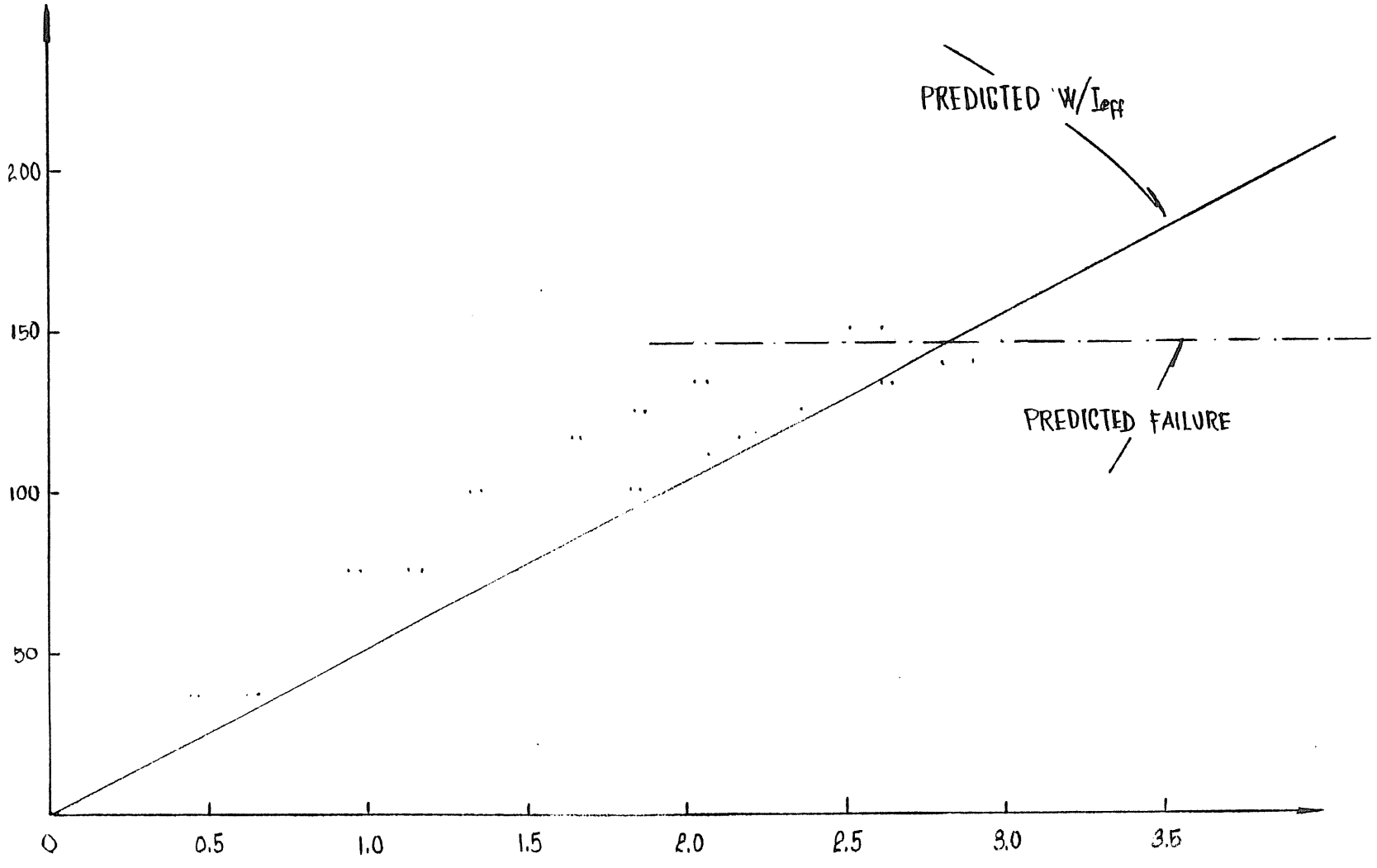

Figure D.2 Load vs. Midspan Deflections, Test 3-1

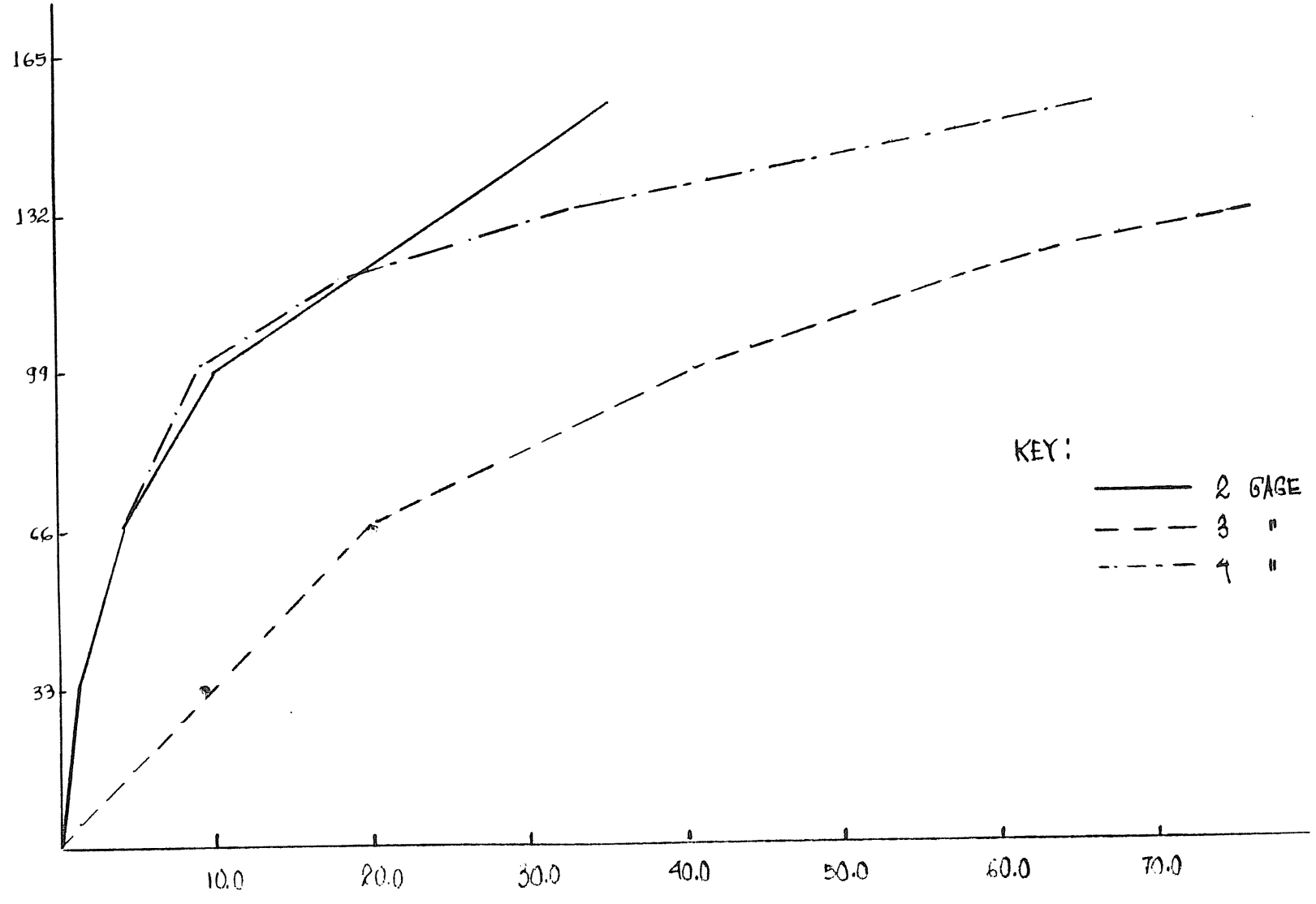

Figure D.3 Load vs. Normal Stress at Lap, Test 3-1

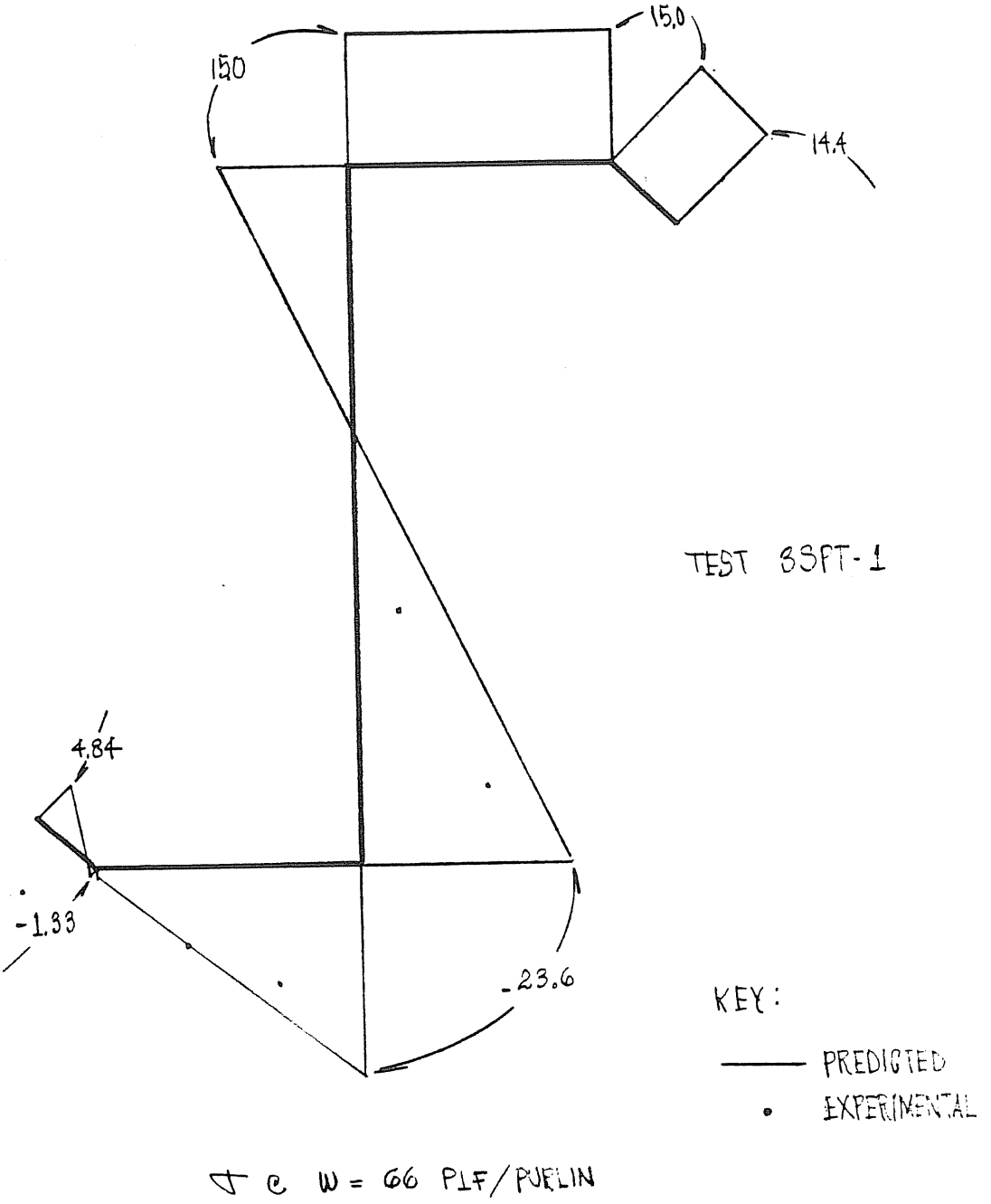

Figure D.4 Stress Distribution at Gaged Section, Test 3-1

APPENDIX E

Test 3-2

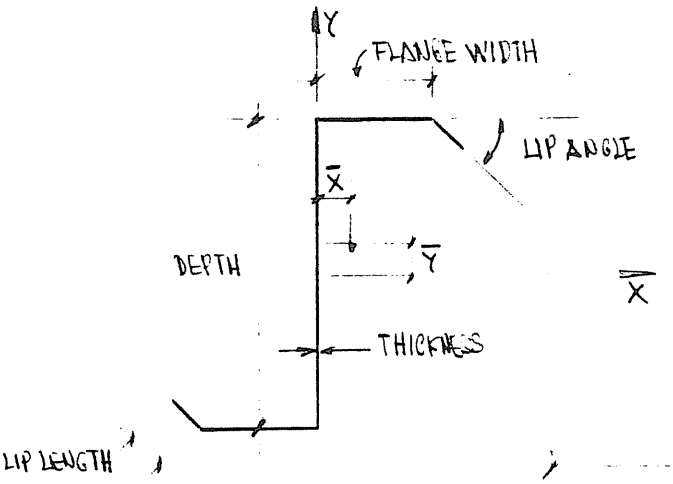

Dimension or Property	
Depth, in.	8.000
Flange Width, in.	2.900
Lip Length, in.	0.650
Thickness, in.	0.067
Lip Angle, deg.	38.50
$\bar{x}$, in.	0.401
$\bar{y}$, in.	0.051
Ixxt, in.^{4}	10.129
Iyyt, in.^{4}	0.792
Ixty, in.^{4}	1.595
Ixyb, in.^{4}	1.106
Yield Stress, ksi	61.260

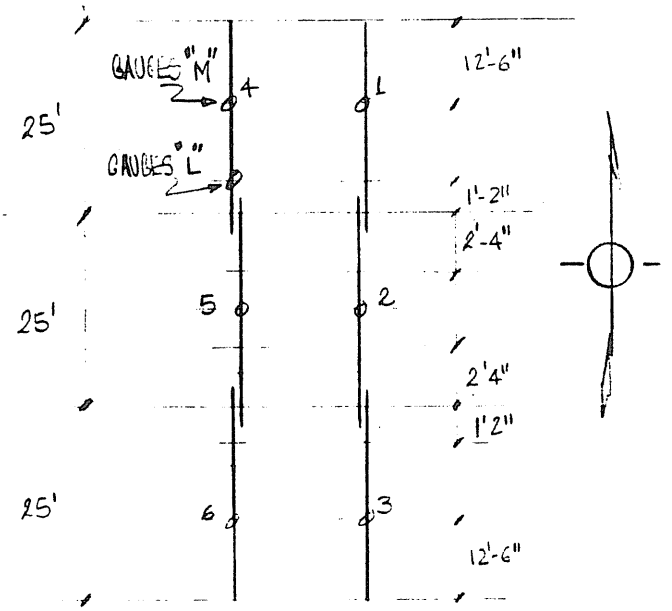

Dial Gauge Locations

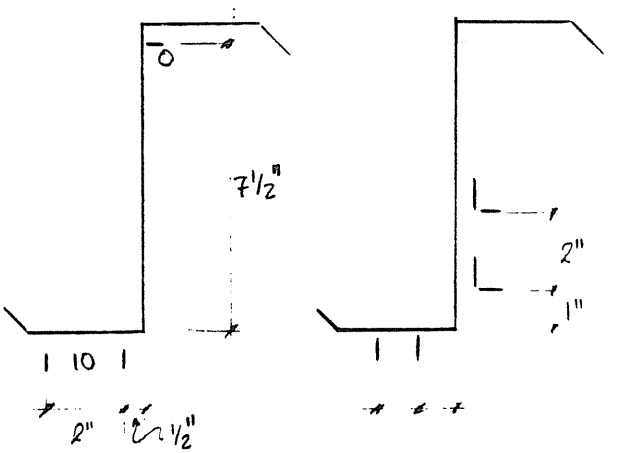

Strain Gauges "M" Strain Gauges "L"

Figure E.1 Section Properties and Instrumentation, Test 3-2

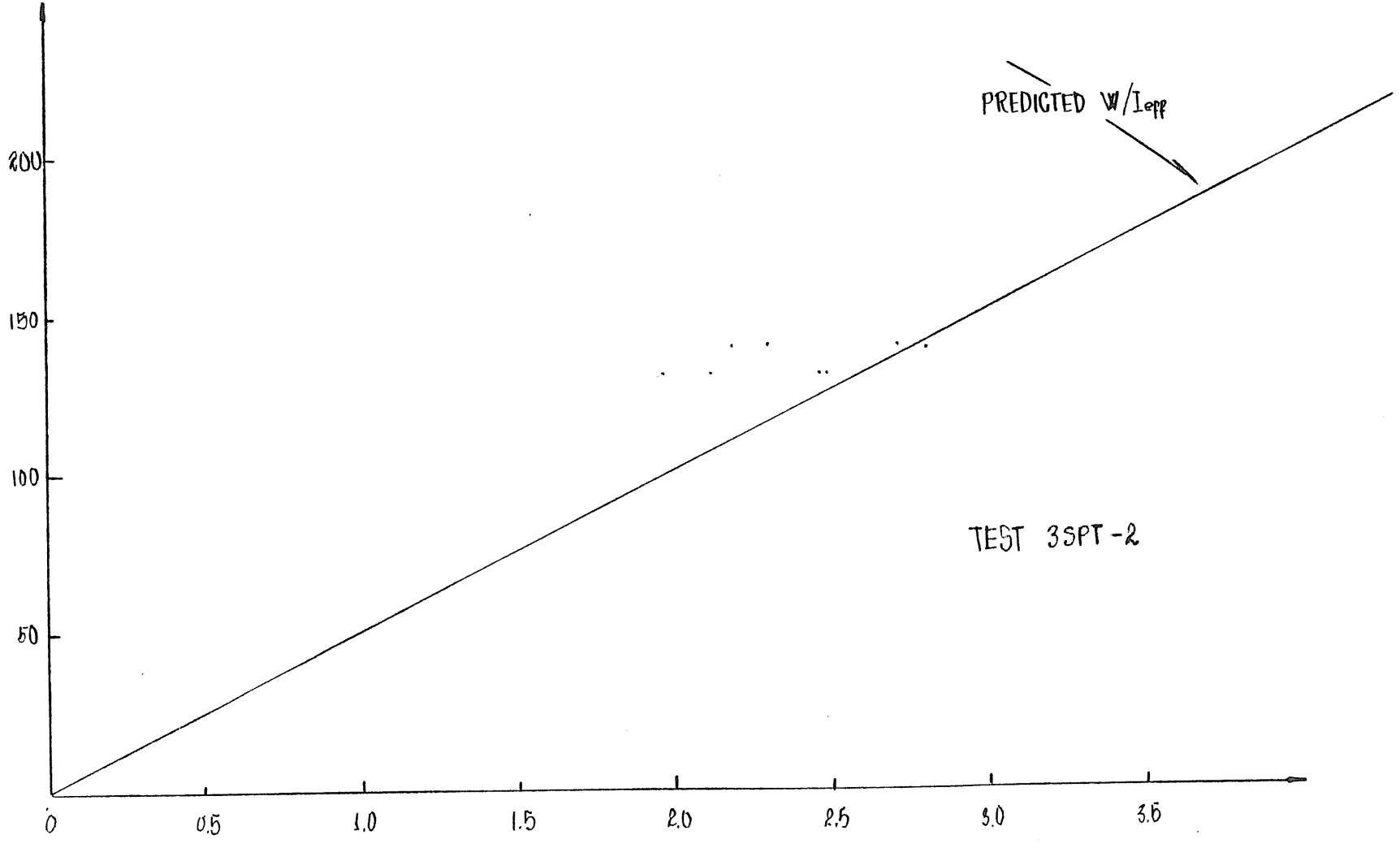

Figure E.2 Load vs. Midspan Deflections, Test 3-2

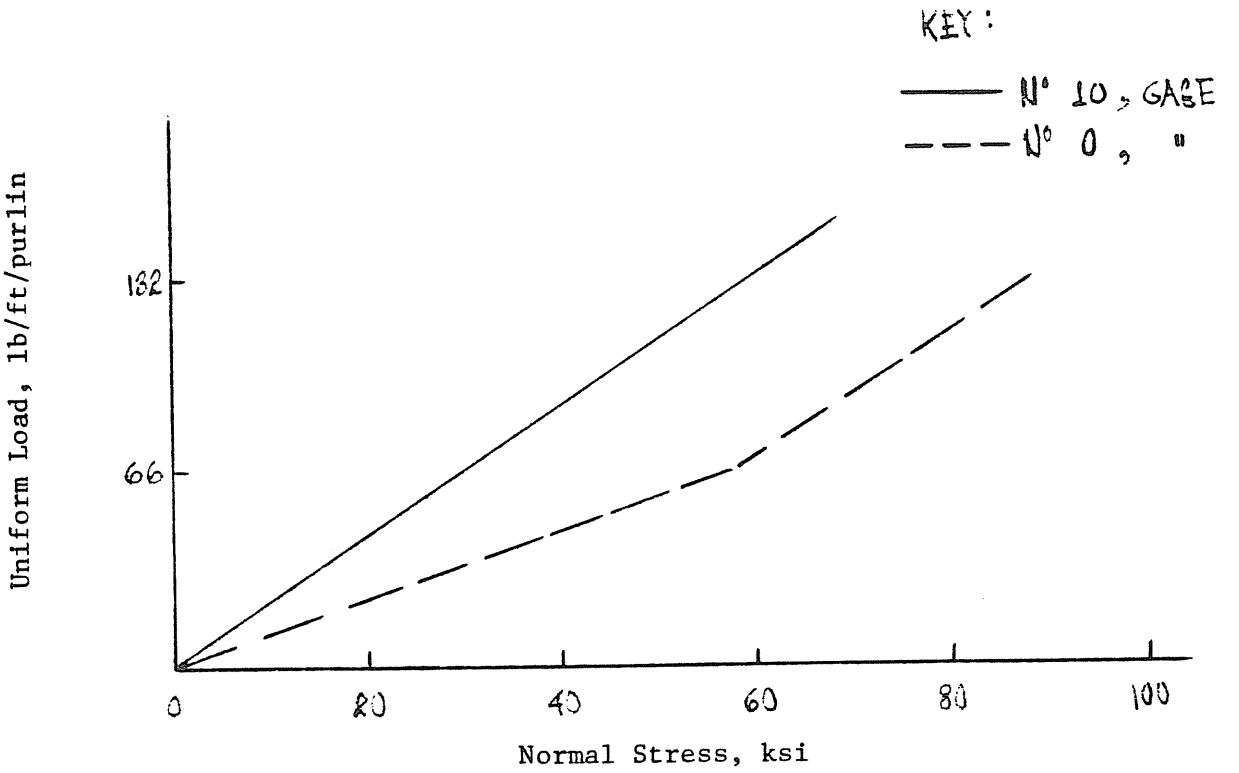

a) Gages 0 and 10

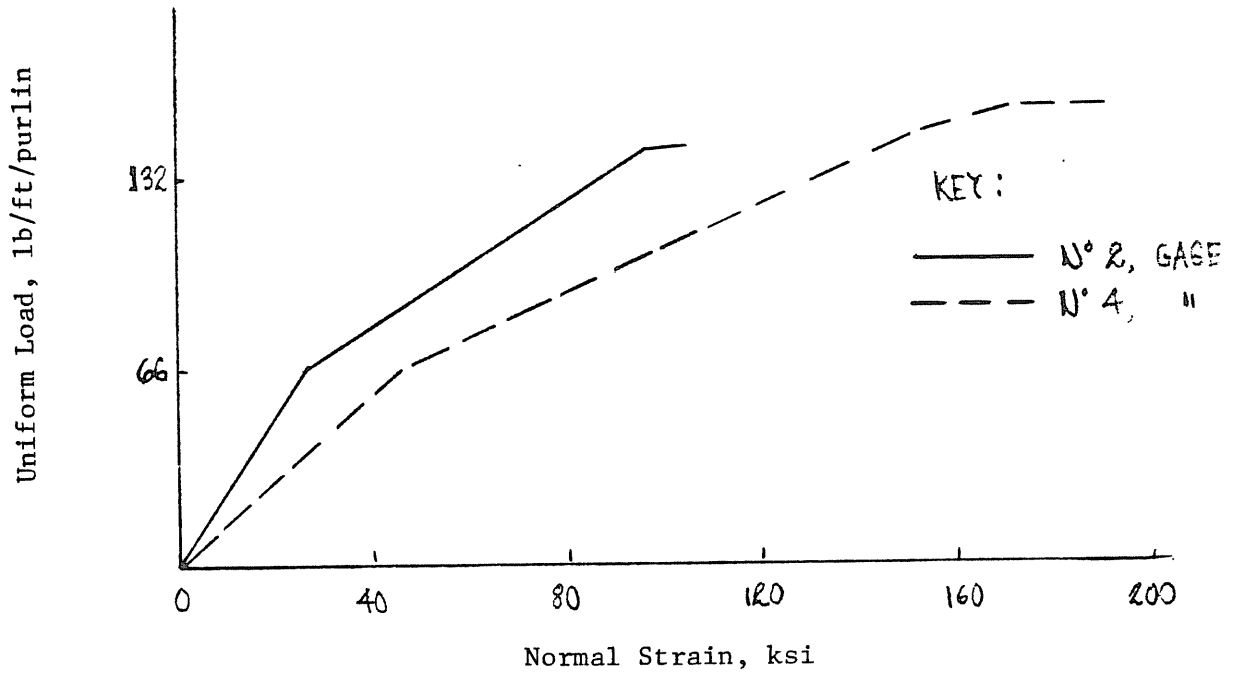

b) Gages 2 and 10

Figure E.3 Load vs. Stress or Strain, Test 3-2

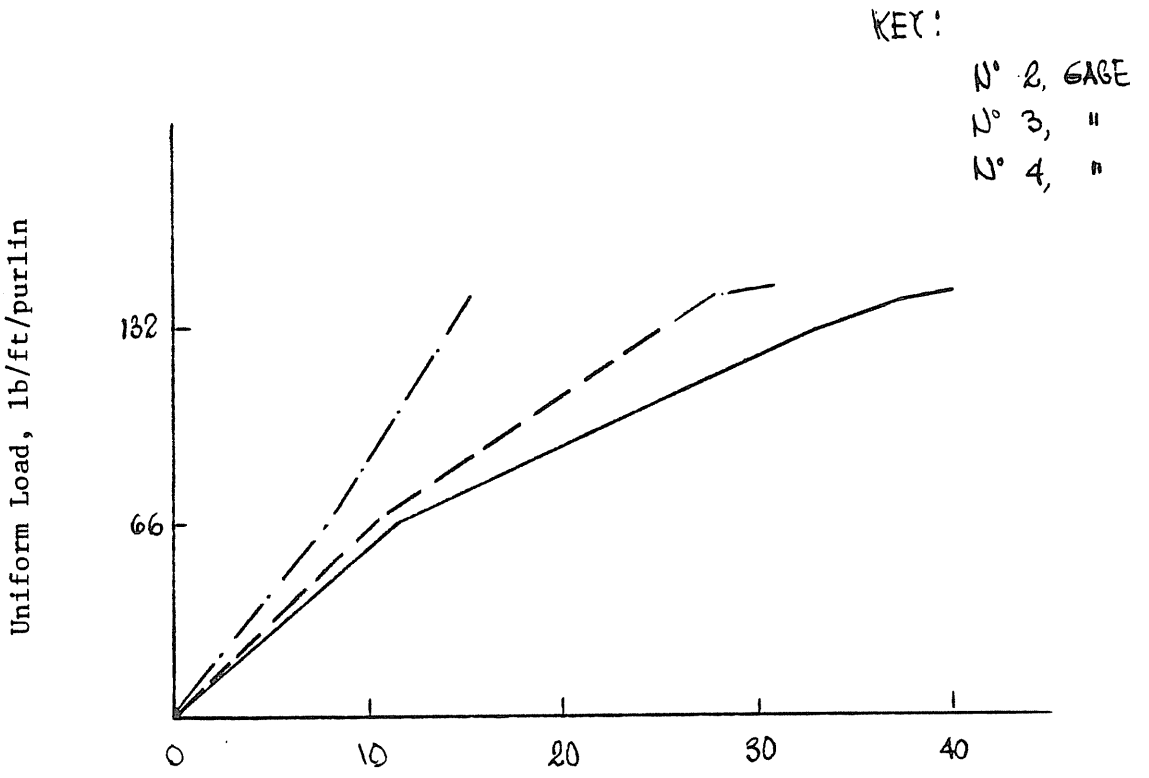

c) Gages 2, 3 and 4

Figure E.3 Continued

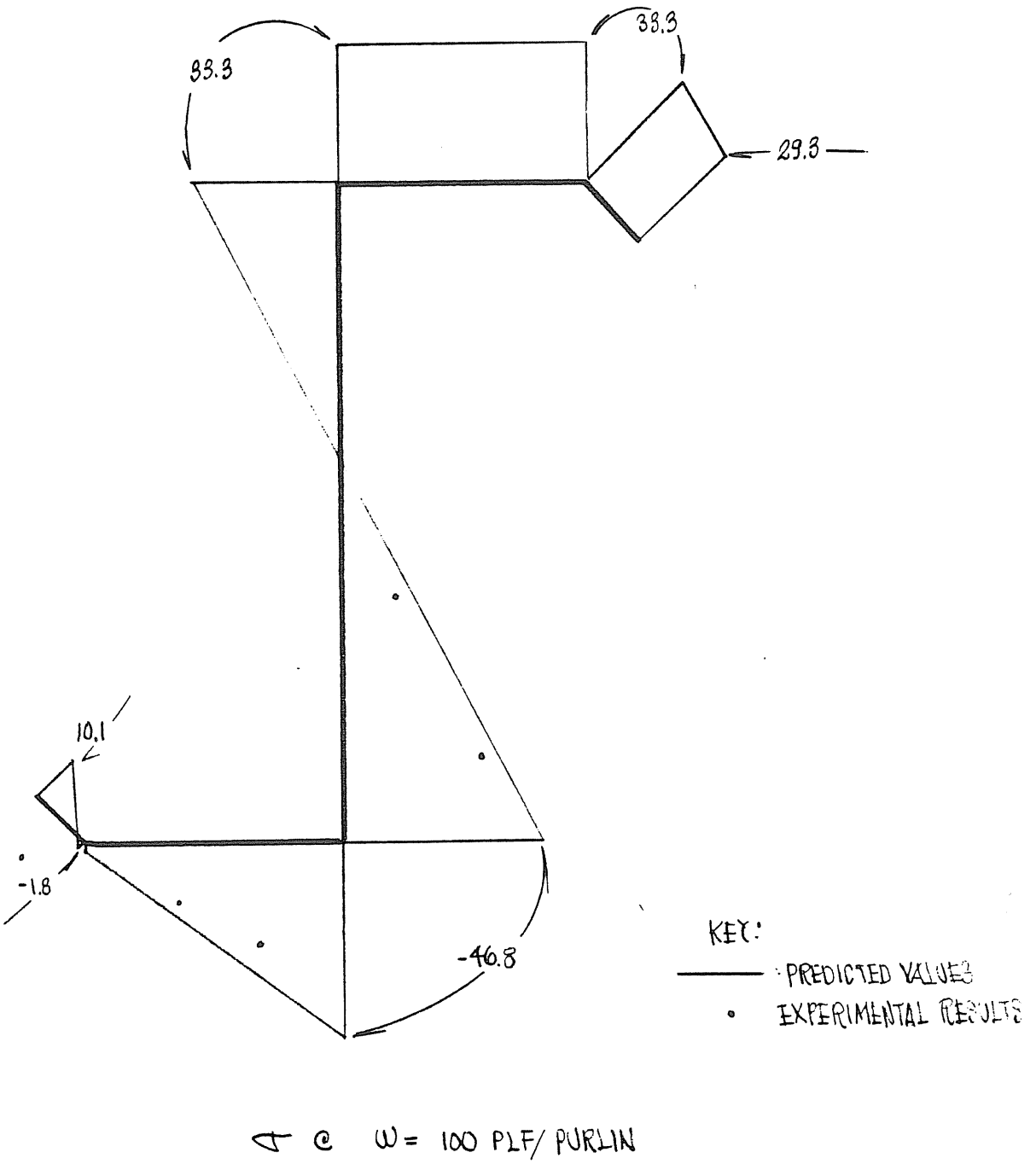

Figure E.4 Stress Distribution at Exterior Lap, Test 3-2

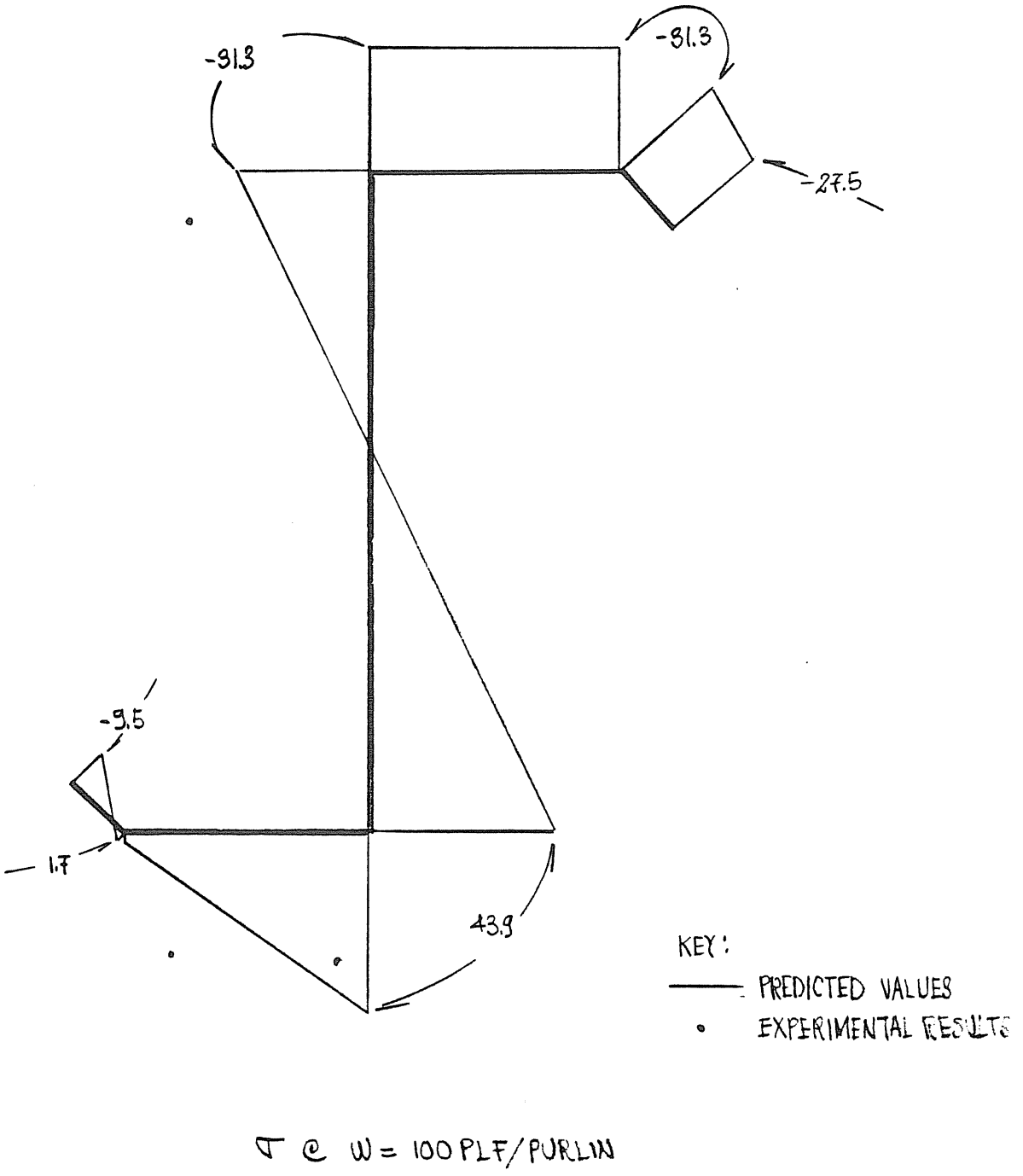

Figure E.5 Stress Distribution at Exterior Midspan, Test 3-2

APPENDIX F

STRUDL Model Data

```
*********************************************************************
*                                                                   *
*  INTEGRATED CIVIL ENGINEERING SYSTEM - IUG VERSION V2M0, JUNE 1976  *
*                          - ICES -                                 *
*            MAY 28, 1980              TIME=13.59.38                *
*                                                                   *
*********************************************************************

STRUDL    '3SPT-2'  'HORIZONTAL WITH ELASTIC FOUNDATION'

          ***********************************************
          *                                             *
          *              ICES STRUDL-II                 *
          *       THE STRUCTURAL DESIGN LANGUAGE        *
          *                                             *
          *        IUG VERSION V3M0,  JUNE 1976         *
          *           SIZE OF POOL  8K BYTES            *
          *             14:01:59       5/28/80         *
          *                                             *
          ***********************************************
TYPE PLANE FRAME
UNITS INCHES KIPS
JOINT COORDINATES
1  0.  0.  S
2  12.  0.  S
3  24.  0.  S
4  36.  0.  S
5  48.  0.  S
6  60.  0.  S
7  72.  0.  S
8  84.  0.  S
9  96.  0.  S
10  108.  0.  S
11  120.  0.  S
12  132.  0.  S
13  144.  0.  S
14  150.  0.
15  156.  0.  S
16  168.  0.  S
17  180.  0.  S
18  192.  0.  S
19  204.  0.  S
20  216.  0.  S
21  228.  0.  S
22  240.  0.  S
23  252.  0.  S
24  264.  0.  S
25  276.  0.  S
26  286.  0.
27  288.  0.  S
28  300.  0.  S
29  312.  0.  S
30  324.  0.  S
31  328.  0.
32  326.  0.  S
33  348.  0.  S
34  360.  0.  S
35  372.  0.  S
36  384.  0.  S
37  396.  0.  S
38  408.  0.  S
39  420.  0.  S
```

```
41  444.  0.  S
42  450.  0.  S
UNITS LBS
JOINT RELEASES
1  28  FORCE X  MOMENT  Z
42  FORCE Y
2  TO  13  15  TO  25  32  TO  41  FORCE X  MOMENT Z  KFY 49.8
27  FORCE X  MOMENT Z  KFY 49.8
29  FORCE X  MOMENT Z KFY 49.8
30  FORCE X  MOMENT Z  KFY 49.8
UNITS KIPS
MEMBER INCIDENCES
1  1  2
2  2  3
3  3  4
4  4  5
5  5  6
6  6  7
7  7  8
8  8  9
9  9  10
10  10  11
11  11  12
12  12  13
13  13  14
14  14  15
15  15  16
16  16  17
17  17  18
18  18  19
19  19  20
20  20  21
21  21  22
22  22  23
23  23  24
24  24  25
25  25  26
26  26  27
27  27  28
28  28  29
29  29  30
30  30  31
31  31  32
32  32  33
33  33  34
34  34  35
35  35  36
36  36  37
37  37  38
38  38  39
39  39  40
40  40  41
41  41  42
CONSTANTS E 29000. ALL
MEMBER PROPERTIES PRISMATIC
1 TO 25  AX 1.0  IZ  0.5876
26  TO  30  AX 2.0  IZ 1.1752
31  TO  41  AX 1.0  IZ  0.5876
UNITS FEET
LOADING  'GRAVITY'
MEMBER 1 TO 41 LOAD FORCE Y UNIFORM W  -0.012
STIFFNESS ANALYSIS
UNITS KIPS INCHES
LIST FOR LOA REA DISP
```

****
RESULTS OF LATEST ANALYSES
****

JOB ID - 3SPT-2 JOB TITLE - HORIZONTAL WITH ELASTIC FOUNDATION

ACTIVE UNITS - LENGTH FORCE ANGLE TEMPERATURE TIME
INCH KIP RAD DEGF SEC

ACTIVE STRUCTURE TYPE - PLANE FRAME

ACTIVE COORDINATES AXES X Y

****
* LOADING - GRAVITY *
****

MEMBER FORCES

MEMBER	JOINT	FORCE			MOMENT		
		AXIAL	SHEAR Y	SHEAR Z	TORSIONAL	BENDING Y	BENDING Z
1	1	0.0	0.0322005				-0.0000000
1	2	0.0	-0.0202005				0.3144054
2	2	0.0	0.0225296				-0.3144054
2	3	0.0	-0.0105296				0.5127609
3	3	0.0	0.0150587				-0.5127609
3	4	0.0	-0.0030587				0.6214653
4	4	0.0	0.0095731				-0.6214653
4	5	0.0	0.0024268				0.6643432
5	5	0.0	0.0058110				-0.6643432
5	6	0.0	0.0061890				0.6620753
6	6	0.0	0.0034908				-0.6620753
6	7	0.0	0.0085092				0.6319650
7	7	0.0	0.0023308				-0.6319650
7	8	0.0	0.0096692				0.5879350
8	8	0.0	0.0020611				-0.5879350
8	9	0.0	0.0099389				0.5406677
9	9	0.0	0.0024292				-0.5406677
9	10	0.0	0.0095708				0.4978183
10	10	0.0	0.0032025				-0.4978183
10	11	0.0	0.0087975				0.4642480
11	11	0.0	0.0041655				-0.4642480
11	12	0.0	0.0078345				0.4422343
12	12	0.0	0.0051172				-0.4422343
12	13	0.0	0.0068827				0.4316413
13	13	0.0	0.0058656				-0.4316413
13	14	0.0	0.0001344				0.4488351
14	14	0.0	-0.0001344				-0.4488351
14	15	0.0	0.0061344				0.4300287
15	15	0.0	0.0062233				-0.4300287
15	16	0.0	0.0057767				0.4327089
16	16	0.0	0.0060041				-0.4327089
16	17	0.0	0.0059959				0.4327577
17	17	0.0	0.0050208				-0.4327577

18	18	0.0	0.0030873	0.4210080
18	19	0.0	0.0089127	0.3860558
19	19	0.0	0.0000229	-0.3860558
19	20	0.0	0.0119771	0.3143310
20	20	0.0	-0.0043373	-0.3143310
20	21	0.0	0.0163373	0.1902836
21	21	0.0	-0.0101270	-0.1902836
21	22	0.0	0.0221270	-0.0032406
22	22	0.0	-0.0174265	0.0032406
22	23	0.0	0.0294265	-0.2843581
23	23	0.0	-0.0262332	0.2843581
23	24	0.0	0.0382332	-0.6711569
24	24	0.0	-0.0364252	0.6711569
24	25	0.0	0.0484252	-1.1802588
25	25	0.0	-0.0477165	1.1802588
25	26	0.0	0.0577165	-1.7074242
26	26	0.0	-0.0577165	1.7074242
26	27	0.0	0.0597165	-1.8248577
27	27	0.0	-0.0596110	1.8248577
27	28	0.0	0.0716110	-2.6121902
28	28	0.0	0.0745676	2.6121902
28	29	0.0	-0.0625676	-1.7893791
29	29	0.0	0.0629528	1.7893791
29	30	0.0	-0.0509528	-1.1059456
30	30	0.0	0.0521020	1.1059456
30	31	0.0	-0.0481020	-0.9055375
31	31	0.0	0.0481020	-0.9055375
31	32	0.0	-0.0461020	0.9997416
32	32	0.0	0.0473967	0.9997416
32	33	0.0	-0.0253967	-0.1990136
33	33	0.0	0.0290886	0.1990136
33	34	0.0	-0.0170886	0.0780497
34	34	0.0	0.0222721	-0.0780497
34	35	0.0	-0.0102721	0.2733154
35	35	0.0	0.0169152	-0.2733154
35	36	0.0	-0.0049152	0.4042973
36	36	0.0	0.0129021	-0.4042973
36	37	0.0	-0.0009021	0.4871227
37	37	0.0	0.0100612	-0.4871227
37	38	0.0	0.0019388	0.5358571
38	38	0.0	0.0081847	-0.5358571
38	39	0.0	0.0038153	0.5620736
39	39	0.0	0.0070437	-0.5620736
39	40	0.0	0.0049563	0.5745986
40	40	0.0	0.0063976	-0.5745986
40	41	0.0	0.0056024	0.5793698
41	41	0.0	0.0060000	-0.5793698
41	42	0.0	-0.0000000	0.5973698

RESULTANT JOINT

SUPPORTS

LOADS -

JOINT		FORCE			MOMENT		
		X FORCE	Y FORCE	Z FORCE	X MOMENT	Y MOMENT	Z MOMENT
1	GLOBAL	0.0	0.0322005				-0.0000000
2	GLOBAL	0.0	0.0023291				0.0000000
3	GLOBAL	0.0	0.0045291				0.0000000
4	GLOBAL	0.0	0.0065144				0.0000000
5	GLOBAL	0.0	0.0082378				0.0000000

6	GLOBAL	0.0	0.0096798		0.0000000
7	GLOBAL	0.0	0.0108400		0.0000000
8	GLOBAL	0.0	0.0117302		-0.0000000
9	GLOBAL	0.0	0.0123682		-0.0000000
10	GLOBAL	0.0	0.0127732		-0.0000000
11	GLOBAL	0.0	0.0129631		0.0000000
12	GLOBAL	0.0	0.0129517		-0.0000000
13	GLOBAL	0.0	0.0127484		-0.0000000
15	GLOBAL	0.0	0.0123577		0.0000000
16	GLOBAL	0.0	0.0117807		-0.0000000
17	GLOBAL	0.0	0.0110168		-0.0000000
18	GLOBAL	0.0	0.0100665		0.0000000
19	GLOBAL	0.0	0.0089356		0.0000000
20	GLOBAL	0.0	0.0076398		-0.0000000
21	GLOBAL	0.0	0.0062103		-0.0000000
22	GLOBAL	0.0	0.0047005		-0.0000000
23	GLOBAL	0.0	0.0031932		-0.0000000
24	GLOBAL	0.0	0.0018080		-0.0000000
25	GLOBAL	0.0	0.0007087		0.0000000
27	GLOBAL	0.0	0.0001055		-0.0000000
28	GLOBAL	0.0	0.1461786		0.0000000
29	GLOBAL	0.0	0.0003852		0.0000000
30	GLOBAL	0.0	0.0011492		-0.0000000
32	GLOBAL	0.0	0.0012947		-0.0000000
33	GLOBAL	0.0	0.0036919		-0.0000000
34	GLOBAL	0.0	0.0051835		0.0000000
35	GLOBAL	0.0	0.0066430		0.0000000
36	GLOBAL	0.0	0.0079869		0.0000000
37	GLOBAL	0.0	0.0091591		-0.0000000
38	GLOBAL	0.0	0.0101235		0.0000000
39	GLOBAL	0.0	0.0108590		-0.0000000
40	GLOBAL	0.0	0.0113539		0.0000000
41	GLOBAL	0.0	0.0116024		-0.0000000
42	GLOBAL	0.0	-0.0000000		0.5973698

RESULTANT JOINT FREE JOINTS LOADS -

JOINT		FORCE			MOMENT		
		X FORCE	Y FORCE	Z FORCE	X MOMENT	Y MOMENT	Z MOMENT
14	GLOBAL	0.0	-0.0000000				-0.0000000
26	GLOBAL	0.0	-0.0000000				-0.0000000
31	GLOBAL	0.0	0.0000000				-0.0000000

RESULTANT JOINT SUPPORTS DISPLACEMENTS -

JOINT		DISPLACEMENT			ROTATION		
		X DISP.	Y DISP.	Z DISP.	X ROT.	Y ROT.	Z ROT.
1	GLOBAL	0.0	0.0				-0.0039386
2	GLOBAL	0.0	-0.0467700				-0.0038195
3	GLOBAL	0.0	-0.0909452				-0.0035198
4	GLOBAL	0.0	-0.1308122				-0.0031120

6	GLOBAL	0.0	-0.1943734	-0.0021753
7	GLOBAL	0.0	-0.2176711	-0.0017112
8	GLOBAL	0.0	-0.2355465	-0.0012732
9	GLOBAL	0.0	-0.2483568	-0.0008674
10	GLOBAL	0.0	-0.2564905	-0.0004933
11	GLOBAL	0.0	-0.2603028	-0.0001461
12	GLOBAL	0.0	-0.2600744	0.0001816
13	GLOBAL	0.0	-0.2559914	0.0004977
15	GLOBAL	0.0	-0.2481468	0.0008095
16	GLOBAL	0.0	-0.2365607	0.0011218
17	GLOBAL	0.0	-0.2212204	0.0014350
18	GLOBAL	0.0	-0.2021382	0.0017440
19	GLOBAL	0.0	-0.1794295	0.0020366
20	GLOBAL	0.0	-0.1534089	0.0022917
21	GLOBAL	0.0	-0.1247043	0.0024778
22	GLOBAL	0.0	-0.0943882	0.0025521
23	GLOBAL	0.0	-0.0641214	0.0024593
24	GLOBAL	0.0	-0.0363050	0.0021313
25	GLOBAL	0.0	-0.0142311	0.0014879
27	GLOBAL	0.0	-0.0021179	0.0005419
28	GLOBAL	0.0	0.0	-0.0002351
29	GLOBAL	0.0	-0.0077346	-0.0010058
30	GLOBAL	0.0	-0.0230773	-0.0015113
32	GLOBAL	0.0	-0.0259977	-0.0017410
33	GLOBAL	0.0	-0.0741339	-0.0024627
34	GLOBAL	0.0	-0.1040868	-0.0024969
35	GLOBAL	0.0	-0.1333939	-0.0023647
36	GLOBAL	0.0	-0.1603805	-0.0021177
37	GLOBAL	0.0	-0.1839170	-0.0017954
38	GLOBAL	0.0	-0.2032837	-0.0014267
39	GLOBAL	0.0	-0.2180524	-0.0010317
40	GLOBAL	0.0	-0.2279891	-0.0006230
41	GLOBAL	0.0	-0.2329798	-0.0002082
42	GLOBAL	0.0	-0.2336076	0.0

RESULTANT JOINT

FREE JOINTS

DISPLACEMENTS -

JCINT		DISPLACEMENT			ROTATION		
		X DISP.	Y DISP.	Z DISP.	X ROT.	Y ROT.	Z ROT.
14	GLOBAL	0.0	-0.2525401				0.0006538
26	GLOBAL	0.0	-0.0033064				0.0006455
31	GLOBAL	0.0	-0.0293659				-0.0016291

FINISH

GOOD-BYE